Table 2. Frequency distribution of N119, D125, E187, G222, and R223 variants within the HA receptor binding site of viruses obtained from clinical specimens infected with influenza A viruses.

	Specimen	Total read	K119N (%)	N125D (%)	D187E (%)	D222G (%)	Q223R (%)
H1N1pdm	#1	3,308	8.59	4.99	0.15	0.74	4.64
1st wave	#2	29,607	4.61	1.01	0.72	21.49	2.39
(2009)	#3	15,514	3.45	4.88	0	3.16	3.62
H1N1pdm	#4	15,485	0.00	1.07	0	0.04	0.57
2nd wave	#5	25,429	0.00	1.33	0	0.02	0.53
(2010)	#6	14,183	0.02	2.15	0	0.07	0.47
	#7	18,046	0.01	1.87	0	0.01	0.63
	#8	11,179	3.10	0.66	0	0.05	0.48
H1N1	#9	2,014	0.00	0.00	0	0.1	0.1
Seasonal	#10	7,170	0.00	0.00	0	0.04	0.15
(2008)	#11	3,652	0.00	0.00	0	0.08	0.16
	#12	3,733	0.00	0.00	0	0.11	0.13
	#13	7,268	0.00	0.00	0	0.01	0.41
Plasmid (control)		12,428	0.00	0.00	0	0	0.38

doi:10.1371/journal.pone.0030946.t002

D222G and/or Q223R substitutions were detected at even higher rates in the early passaged (P1) viruses (Table 3) than in the parental viruses (Table 1). More than half (98.6%, 95.0%, and 59.7% in #1, #2, and #3, respectively) possessed either D222G or Q223R substitutions (Table 3). K119N, N125D and D187E mutations were also detected at higher ratios in the P5 or P6 passages than in the P1 passage, suggesting that these mutations were being selected for effective growth in avian cells. We also detected these substitutions at a lower level in the MDCK-passaged viruses compared with the egg-passaged viruses (Table 3). In contrast to the HA gene, no amino acid substitutions were detected in the RNA polymerase B2 (PB2), RNA polymerase B1 (PB1 and PB1-F2), RNA polymerase A (PA), neuraminidase (NA), matrix proteins (M1 and M2) and non-structural proteins (NS1 and NS2) of the P5/P6 viruses compared with the nucleotide sequence of the original H1N1pdm derived from the #2 clinical specimen (data not shown).

P5/P6 in #1, #2, and #3 specimens reduced hemagglutination titers when RBCs were treated with α2,3 sialidase whereas the titers did not change in MDCK-passaged viruses (Table 4). These results suggested that egg-passaged viruses, including G222 and/or R223, were α2,3 sialic acid receptor tropic and that MDCK-passaged viruses including D222 and Q223 had α2,6 sialic acid receptor specificity. From these results, we can extrapolate that the major populations in the original specimens #1–#3 had α2,6 sialic acid receptor tropism. These results are coincident with the homology modeling and docking of D222G and Q223R mutants (Figure S4).

Deep sequencing analysis of H1N1pdm HA D222G or Q223R mutants from the second wave of the outbreak

To elucidate the transmissibility of the G222 and/or R223 viruses in humans, five nasal swabs (#4–#8) obtained from individuals with a mild case of H1N1pdm in December 2010 were examined by deep sequencing analysis. The same region of HA RBS (369 bp) as shown in Figure 1 was amplified by One Step RT-PCR. The results showed

Table 3. Frequency of amino acid mutations in the hemagglutinin receptor binding site in egg-passaged or MDCK-passaged samples.

Specimen	Isolation	Total Read	Mutant Ratio (%)				
			K119N	N125D	D187E	D222G	Q223R
#1	P1	495	0.6	0.2	0	3	95.6
	P6	330	0	96.7	12.1	7.9	95.8
	MDCK	481	0.2	0.8	1.5	1.9	2.7
#2	P1	340	0.6	12.1	0.3	24.4	70.6
	P6	202	60.4	33.7	25.7	60.4	33.2
	MDCK	515	0	0	0	0.4	0
#3	P1	300	0.7	0	0	59	0.7
	P5	193	49.2	36.3	0	85	0.5

doi:10.1371/journal.pone.0030946.t003

that, by December 2010, both the G222 and R223 variants had almost disappeared (0.01–0.07% and 0.47–0.63%, respectively) (Table 2). The K119N mutation frequency also shifted to an undetectable level except for one specimen (#8). By contrast, the N125D mutation could still be detected (0.66–2.15%; average, 1.42%) (Table 2). Taken together, these results suggest that the H1N1pdm D222 and Q223 variants are competent for human-to-human transmission but that the α2,3 sialic acid-specific G222 and R223 mutations resulted in low transmissibility. We also examined the substitution rates in seasonal H1N1 viruses using five nasal swabs (#9–#13) from patients diagnosed in 2008 (Table 2). The results showed low substitution rates for D222G and Q223R (0.01–0.11% and 0.1–0.41%, respectively), consistent with the results of the second epidemic, in H1N1pdm.

Discussion

This study used a high-throughput sequencing approach to analyze more than 2,000 clones from each of eight H1N1pdm samples obtained in 2009–2010. The results showed that α2,3 sialic acid-specific viruses containing D222G and/or Q223R substitutions within the HA molecule were present in the upper respiratory tract as a minor population in patients with mild H1N1pdm infections in the early phase (May 2009) of the pandemic in Japan. However, these substitutions nearly disappeared in the samples from five mild cases in Dec 2010, suggesting that the D222G and/or

Table 4. Hemagglutination assay using chicken, guinea pig, and horse erythrocytes with or without α2,3 sialidase treatment.

	Chicken		Guinea pig		Horse	
α2,3 sialidase	−	+	−	+	−	+
#1-P6	512	8	1,024	32	128	16
#2-P6	512	256	512	1,024	64	4>
#3-P5	256	128	512	512	64	4>
#1-MDCK	256	256	512	1,024	128	128
#2-MDCK	32	16	256	256	8	8

doi:10.1371/journal.pone.0030946.t004

Q223R mutants showed low rates of human-to-human transmission. Thus, the newly emergent influenza A viruses may have been dual specific but not exclusively α2,6-sialic acid-specific during the early phase of the pandemic and adapted during multiple cycles of human-to-human transmission. These results are consistent with previous reports showing that, during previous pandemics, the receptor binding properties of avian influenza viruses changed after introduction into mammals [8]. In particular, positions 187 and 222 within the HA of H1 viruses and position 223 in H2 and H3 strains are critical for receptor binding specificity [8]. In the present study, the D187E substitution was not striking, suggesting that E187 had already disappeared in humans, or the original swine lineages, by May 2009. The N125D mutation, however, was detected (0.66–2.15%), even in the second wave of the outbreak (Table 2). However, as far as we know, there is no report indicating that this mutation affects receptor-binding affinity and specificity. The K119N mutation was also significantly detected in one specimen (3.1%) from a patient who had similar clinical symptoms as those of other patients during the second wave of the outbreak (Table 2). Neither mutation was detected in specimens of seasonal H1N1 in 2008, suggesting that further prospective study, as well as virological study, is required to understand the functions of these mutations.

HA residue 222 plays a critical role in the binding affinity of the galactose moiety of sialosaccharides for the RBS. The D222G mutation would result in a loss of interaction between galactose and K219 (Figure S4) because of the loss of charge and the side-chain. In turn, this would open up a cavity on the side of the RBS to accommodate the α2,3-linked receptor [11,12]. Residue 223 is also important for the binding affinity of galactose and the terminal sialic acid of the receptor. The emergence of a positively charged and bulky Arginine(R) instead of Glutamine(Q) at this position would disturb the interaction between K219 and galactose, leading to decreased virus affinity for the α2,6-linked receptor (Figure S4) [13,14]. Also, the homology modeling results showed that the double mutations, D187E and Q223R, would decrease virus affinity for the α2,6-linked receptor because the salt-bridge between E187 and R223 would lead to narrowing of the receptor binding pocket (data not shown).

In this study, we performed deep amplicon sequencing using Roche/454 GS-Junior technology. We compared the results obtained by using deep sequencer with those obtained by the conventional Sanger method to evaluate this newly developed technology. Sequencing analysis using next-generation technology is necessary to reveal H1N1pdm genetic diversity in detail; our preliminary sequencing analysis using a conventional cloning approach failed to detect the D222G mutation in specimen #1 (Figure 1 and Table 2). The frequency of mutations such as D187E in specimens #1 and #2 and D222G in specimen #2 was not the same between GS-Junior technology and conventional Sanger sequencing (Figures 1, S1, S2, and S3, Tables 1 and 2). This discrepancy might be due to the different number of clones sequenced in each method. The proportion of HA sequences observed with D222G and Q223R in the #1 and #2 P6 and in the #3 P5 PCR products (Table 3) was consistent with results obtained by direct sequencing analysis using the ABI Sanger sequencer (Figure S6), suggesting that high-throughput amplicon sequencing analysis was highly quantitative.

The present study did not confirm whether viruses with the D222G and/or Q223R substitutions actually replicated in humans; however, the D222G and Q223R mutant viruses formed the dominant population when specimens were inoculated into embryonic chicken eggs (Table 3), indicating that the G222 and R223 mutants may be able to replicate in humans.

Several reports have shown that the D222G substitution was associated with severe, and sometimes fatal, cases of H1N1pdm [10,15,16,17,18]. It has also been reported that two different amino acids, D and E, may be polymorphic variants at position 222 [19], and that amino acids, G or N, would be present in potentially more pathogenic mutants or circulating variants [20]. However, the relevance of the mutation at position 222 to H1N1pdm pathogenesis remains unclear. In this study, D222E, D222N, and D222V variants were not detected, even when deep sequencing was performed (Table S1). D222G mutants were detected as a minor population even in mild cases; thus, every patient may have been exposed to D222G mutant viruses. Minority α2,3 sialic acid-tropic G222 mutants could be amplified in α2,3 sialic acid expressing cells in the lower respiratory tract of certain populations, which would result in severe to fatal respiratory illness in these populations. No conclusions can be drawn regarding the relationship between the D222G substitution and pathogenesis from the present study. Therefore, further study is required to determine whether G222 viruses were ever present as a major population in the lower respiratory tract of patients with severe or fatal pneumonia due to H1N1pdm infection.

Materials and Methods

Clinical samples

Three and five individual H1N1pdm-positive nasal swabs were provided in May 2009 and December 2010, respectively, in Osaka, Japan. All of the patients examined in 2009 had fever, sore throat, and cough, but were not hospitalized. They were administered oseltamivir after nasal swab-sampling. The patients examined in 2010 had upper respiratory symptoms but were not hospitalized. As a control, five specimens diagnosed with seasonal H1N1 in 2008 in Osaka were investigated. The analyzed samples were unlinked and anonymous in the Osaka Prefectural Institute of Public Health. This study was approved by the ethical review committees of the Osaka Prefectural Institute of Public Health and the Research Institute for Microbial Diseases (RIMD), Osaka University. The Both ethical committees specifically waived the need for consent.

RNA extraction

Each nasal swab was collected in Hanks solution and was centrifuged at 20,000 *g* for 10 min. The supernatants were suspended in TRIzol LS reagent (Life Technologies/Invitrogen, Carlsbad, USA) for 60 min. Total RNA was extracted using a PureLink™ RNA Mini Kit (Life Technologies/Invitrogen) according to the manufacturer's instructions. Contaminating DNA was eliminated with DNAase I (Life Technologies/Invitrogen).

One-step reverse transcription-PCR (RT-PCR)

Total RNA was subjected to One-step RT-PCR (SuperScript III/Platinum Taq HiFi One-step RT-PCR Kit; (Life Technologies/Invitrogen) to detect the receptor binding site in the HA molecule. The primers used were as follows: forward primer, $5'\text{-}_{416}$TTGAAAGGTTTGAGATATTC$_{435}$-3′; reverse primer, $5'\text{-}_{784}$CTAGTGTCCAGTAATAGTTC$_{765}$-3′.

Plasmid cloning

Amplified PCR products were cloned into the pGEM-T easy vector (Promega, Madison, WI). More than one hundred clones per specimen (109, 103, and 101 clones in #1, #2, and #3, respectively) were sequenced using conventional Sanger technology (Life technologies/Applied Biosystems, Carlsbad, USA).

Virus isolation and serial passage in embryonated eggs and Madin-Darby canine kidney (MDCK) cells

Clinical specimens were injected into 9-day-old embryonated chicken eggs for virus isolation [21]. After incubation at 37°C for 72 h, the allantoic fluids were collected and filtered (Passage 0: P0). The samples were then diluted 1–100 fold in phosphate buffered saline (PBS) and passaged either six (samples derived from #1 and #2) or five (sample derived from #3) times in embryonated chicken eggs. Identical specimens derived from #1 and #2 were also inoculated into MDCK cells for virus isolation [22] and the amplified viruses were serially passaged two or three times in MDCK cells.

Hemagglutination titration

Viral samples were serially diluted with PBS and added at a concentration of 0.5% to chicken red blood cells. After incubation at room temperature for 30 min, hemagglutination was observed.

High-throughput pyrosequencing and data analysis

PCR products were purified using the QIAquick® PCR purification kit (Qiagen GmbH, Hilden, Germany) and were ligated with RL MID adaptors (Roche Diagnostics GmbH, Mannheim, Germany). The PCR products were further purified with Agencourt AMPure XP beads (Beckman Coulter, Brea, USA). The quality and quantity of the library was assessed using an Agilent 2100 Bioanalyzer (Agilent Technologies, Santa Clara, USA) and TBS380 mini fluorometer (A. Daigger & Company Inc., Vernon Hills, USA), respectively. After amplifying the samples by emulsion PCR, high-throughput pyrosequencing was performed using a GS Junior (Roche Diagnostics GmbH). Data analysis was performed on each sequence read using computational tools as described previously [23,24,25].

α2,3 sialidase treatment

100 μl of 10% chicken, guinea pig, or horse red blood cells were treated with 10 U of α2,3 sialidase (New England Biolabs, Ipswich, MA) at 37°C for 18 h and were washed with PBS. After the erythrocyte suspension was diluted to 0.5% (chicken) or 0.75% (guinea pig and horse), the hemagglutination titer was measured as described above.

Homology modeling and docking

The crystal structure of HA of influenza virus, A/Brevig Mission/1/1918 (H1N1) (Protein Data Bank ID code 2WRG), was used as a template for homology modeling by using a Molecular Operating Environment. SA α2,6-linked structural analogs were used as inputs for docking with the model HA structure.

Supporting Information

Figure S1 Alignment of the amino acid sequences within the receptor binding site of variants other than E187, G222, and R223. Variants other than E187, G222, and R223 (Figure 1) obtained from clinical specimen #1 from the first wave of the outbreak.
(TIFF)

Figure S2 Alignment of the amino acid sequences within the receptor binding site of variants other than E187, G222, and R223. Variants other than E187, G222, and R223 (Figure 1) obtained from clinical specimen #2 from the first wave of the outbreak.
(TIFF)

Figure S3 Alignment of the amino acid sequences within the receptor binding site of variants other than E187, G222, and R223. Variants other than E187, G222, and R223 (Figure 1) obtained from clinical specimen #3 from the first wave of the outbreak.
(TIFF)

Figure S4 Stereo views of the homology-based structural model for binding of sialosaccharides to the RBS of H1N1pdm hemagglutinin. The structural complex of the RBS of H1N1pdm HA with human receptor (orange) was constructed using the co-crystal structure of A/Brevig Mission/1/1918 (PDB ID: 2WRG) as a template. (A) HA of wild type (pink) overlapped with the HA of D222G mutants (green). Position 222 is shown in deep colors. Putative interactions salt-bridge between the sugar and the RBS are shown as black dashed lines. (B) HA of wild type (pink) overlapped with the HA of Q223R mutants (blue). Q223 and R223 are shown in deep pink and yellow, respectively.
(TIFF)

Figure S5 Kinetics of hemagglutination in viruses isolated from egg-passaged samples (#1, #2, and #3). Clinical specimens were injected into 9-day-old embryonated chicken eggs and incubated for 72 h. Allantoic fluid was collected (passage 0) and serially passaged in chicken eggs (passage 5–6). The viral growth of each sample was measured by hemagglutination assay using (0.5%) chicken red blood cells.
(TIFF)

Figure S6 Direct sequencing analysis of PCR products (positions 221–227 aa in HA-RBS) amplified from egg-passaged P6 (#1 and #2) and P5 (#3) viruses using a conventional ABI sequencer. The arrows indicate nucleotide substitutions. WT indicates wild type.
(TIFF)

Table S1 Frequency distribution of D222G, D222N, D222V, and D222E variants within the hemagglutinin receptor binding site of viruses obtained from clinical specimens (#1–#3).
(TIFF)

Acknowledgments

We are grateful to R. Koketsu, Y. Watanabe, N. Higashi, S. Morikawa, S. Hiroi, T. Kase, M. Tujikawa, M. Yunoki, S. Yoshiki, and A. Yoshioka for technical support and to Y. Okuno for helpful discussions.

Author Contributions

and designed the experiments: MY SN TN. Performed the experiments: MY C-SY TD RR TN. Analyzed the data: MY SN NK KI TN. Contributed reagents/materials/analysis tools: TY TI TH KT. Wrote the paper: MY TN.

References

1. Miller MA, Viboud C, Balinska M, Simonsen L (2009) The signature features of influenza pandemics–implications for policy. N Engl J Med 360: 2595–2598.
2. Neumann G, Noda T, Kawaoka Y (2009) Emergence and pandemic potential of swine-origin H1N1 influenza virus. Nature 459: 931–939.
3. Ikonen N, Haanpaa M, Ronkko E, Lyytikainen O, Kuusi M, et al. (2010) Genetic diversity of the 2009 pandemic influenza A(H1N1) viruses in Finland. PLoS One 5: e13329.
4. Kuroda M, Katano H, Nakajima N, Tobiume M, Ainai A, et al. (2010) Characterization of quasispecies of pandemic 2009 influenza A virus (A/H1N1/2009) by de novo sequencing using a next-generation DNA sequencer. PLoS One 5: e10256.
5. Puzelli S, Facchini M, Spagnolo D, De Marco MA, Calzoletti L, et al. (2010) Transmission of hemagglutinin D222G mutant strain of pandemic (H1N1) 2009 virus. Emerg Infect Dis 16: 863–865.

6. Chutinimitkul S, Herfst S, Steel J, Lowen AC, Ye J, et al. (2010) Virulence-associated substitution D222G in the hemagglutinin of 2009 pandemic influenza A(H1N1) virus affects receptor binding. J Virol 84: 11802–11813.
7. Liu Y, Childs RA, Matrosovich T, Wharton S, Palma AS, et al. (2010) Altered receptor specificity and cell tropism of D222G hemagglutinin mutants isolated from fatal cases of pandemic A(H1N1) 2009 influenza virus. J Virol 84: 12069–12074.
8. Matrosovich M, Tuzikov A, Bovin N, Gambaryan A, Klimov A, et al. (2000) Early alterations of the receptor-binding properties of H1, H2, and H3 avian influenza virus hemagglutinins after their introduction into mammals. J Virol 74: 8502–8512.
9. Tumpey TM, Maines TR, Van Hoeven N, Glaser L, Solorzano A, et al. (2007) A two-amino acid change in the hemagglutinin of the 1918 influenza virus abolishes transmission. Science 315: 655–659.
10. Chen Z, Wang W, Zhou H, Suguitan AL, Jr., Shambaugh C, et al. (2010) Generation of live attenuated novel influenza virus A/California/7/09 (H1N1) vaccines with high yield in embryonated chicken eggs. J Virol 84: 44–51.
11. Nunthaboot N, Rungrotmongkol T, Malaisree M, Kaiyawet N, Decha P, et al. (2010) Evolution of human receptor binding affinity of H1N1 hemagglutinins from 1918 to 2009 pandemic influenza A virus. J Chem Inf Model 50: 1410–1417.
12. Stevens J, Blixt O, Glaser L, Taubenberger JK, Palese P, et al. (2006) Glycan microarray analysis of the hemagglutinins from modern and pandemic influenza viruses reveals different receptor specificities. J Mol Biol 355: 1143–1155.
13. Mochalova L, Gambaryan A, Romanova J, Tuzikov A, Chinarev A, et al. (2003) Receptor-binding properties of modern human influenza viruses primarily isolated in Vero and MDCK cells and chicken embryonated eggs. Virology 313: 473–480.
14. Viswanathan K, Chandrasekaran A, Srinivasan A, Raman R, Sasisekharan V, et al. (2010) Glycans as receptors for influenza pathogenesis. Glycoconj J 27: 561–570.
15. Chan PK, Lee N, Joynt GM, Choi KW, Cheung JL, et al. (2011) Clinical and virological course of infection with haemagglutinin D222G mutant strain of 2009 pandemic influenza A (H1N1) virus. J Clin Virol 50: 320–324.
16. Chen H, Wen X, To KK, Wang P, Tse H, et al. (2010) Quasispecies of the D225G substitution in the hemagglutinin of pandemic influenza A(H1N1) 2009 virus from patients with severe disease in Hong Kong, China. J Infect Dis 201: 1517–1521.
17. Mak GC, Au KW, Tai LS, Chuang KC, Cheng KC, et al. (2010) Association of D222G substitution in haemagglutinin of 2009 pandemic influenza A (H1N1) with severe disease. Euro Surveill 15: pii19534.
18. Melidou A, Gioula G, Exindari M, Chatzidimitriou D, Diza E, et al. (2010) Molecular and phylogenetic analysis of the haemagglutinin gene of pandemic influenza H1N1 2009 viruses associated with severe and fatal infections. Virus Res 151: 192–199.
19. Ledesma J, Pozo F, Ruiz MP, Navarro JM, Pineiro L, et al. (2011) Substitutions in position 222 of haemagglutinin of pandemic influenza A (H1N1) 2009 viruses in Spain. J Clin Virol 51: 75–78.
20. Valli MB, Selleri M, Meschi S, Zaccaro P, Vincenti D, et al. (2011) Hemagglutinin 222 variants in pandemic (H1N1) 2009 virus. Emerg Infect Dis 17: 749–751.
21. Daidoji T, Koma T, Du A, Yang CS, Ueda M, et al. (2008) H5N1 avian influenza virus induces apoptotic cell death in mammalian airway epithelial cells. J Virol 82: 11294–11307.
22. Ueda M, Daidoji T, Du A, Yang CS, Ibrahim MS, et al. (2010) Highly pathogenic H5N1 avian influenza virus induces extracellular Ca2+ influx, leading to apoptosis in avian cells. J Virol 84: 3068–3078.
23. Nakamura S, Maeda N, Miron IM, Yoh M, Izutsu K, et al. (2008) Metagenomic diagnosis of bacterial infections. Emerg Infect Dis 14: 1784–1786.
24. Nakamura S, Nakaya T, Iida T (2011) Metagenomic analysis of bacterial infections by means of high-throughput DNA sequencing. Exp Biol Med (Maywood) 236: 968–971.
25. Nakamura S, Yang CS, Sakon N, Ueda M, Tougan T, et al. (2009) Direct metagenomic detection of viral pathogens in nasal and fecal specimens using an unbiased high-throughput sequencing approach. PLoS One 4: e4219.

Clinica Chimica Acta 413 (2012) 467–472

Contents lists available at SciVerse ScienceDirect

Clinica Chimica Acta

journal homepage: www.elsevier.com/locate/clinchim

Diagnosis of HIV-1 infection by near-infrared spectroscopy: Analysis using molecular clones of various HIV-1 subtypes

Akikazu Sakudo [a,b,*], Yoshikazu Suganuma [a], Rina Sakima [b], Kazuyoshi Ikuta [a]

[a] Department of Virology, Center for Infectious Disease Control, Research Institute for Microbial Diseases, Osaka University, Yamadaoka 3-1, Suita, Osaka 565-0871, Japan
[b] Laboratory of Biometabolic Chemistry, School of Health Sciences, Faculty of Medicine, University of the Ryukyus, Uehara 207, Nishihara, Okinawa 903-0215, Japan

ARTICLE INFO

Article history:
Received 26 September 2011
Received in revised form 31 October 2011
Accepted 31 October 2011
Available online 11 November 2011

Keywords:
HIV
Near-infrared spectroscopy
PCA
Water

ABSTRACT

Background: Previously, we investigated the possibility of using near-infrared (NIR) spectroscopy for the diagnosis of human immunodeficiency virus type-1 (HIV-1) infection. Here, we further analyze NIR spectra using molecular clones of various HIV-1 subtypes.
Methods: Culture supernatants of pNL4-3- (HIV-1 molecular clone) or pUC18- (empty vector) transfected 293 T cells were used. In addition, culture supernatants obtained using pBal (HIV-1 subtype B molecular clone) or pIndieC (HIV-1 subtype C molecular clone) were used. Near-infrared radiation (NIR) spectra, obtained using the culture supernatants, were subjected to principal component analysis (PCA) to extract and analyze their properties.
Results: The PCA demonstrated that HIV-1 in medium altered wavelength absorption at around 950 and 1030 nm, suggesting that the HIV-1 altered OH vibration in water. In addition, absorption varied among subtypes at around 950, 1030 and 1060 nm, suggesting that the interaction between HIV-1 and water varies among subtypes.
Conclusions: These differences in the NIR spectra may make it possible to delineate HIV-1 subtypes spectroscopically.

1. Introduction

Near-infrared spectroscopy (NIRS) is a spectroscopic method that uses near-infrared radiation (NIR) in the wavelength region of 700–2500 nm [1]. The visible-NIR region of 650–1100 nm is called the "optical window," a region most suitable for the measurement of biological samples [2]. Alterations in biomolecules, such as proteins, lipids and carbohydrates, can be analyzed within the "optical window" [3–9]. Absorption, which occurs in the NIR region, results from the stretching of hydrogen-bonded functional groups (e.g., —CH, —OH, and —NH) and the overtone and combination tone of bending vibration [9]. We previously demonstrated that infection of human immunodeficiency virus type-1 (HIV-1) could be diagnosed by NIRS [10,11]. So far, besides HIV-1, this method can also be used to diagnose the presence of various other viruses including tobacco mosaic virus [12], soybean mosaic virus [13] and fungi viruses [14]. However, the detailed mechanism by which viruses, including HIV-1, alter the NIRS signal is unknown. Here, we have used molecular biological and biochemical techniques to examine how HIV-1 is detected by NIRS and to determine the wavelength of the NIR region for detection of various HIV-1 subtypes.

2. Materials and methods

2.1. Viral vectors

pNL4-3 [15] and pIndieC [16] comprise pUC18 with an insert of HIV-1 subtype B gene, pBal (subtype B, supplied by Masashi Tatsumi, National Institute of Infectious Diseases) or HIV-1 subtype C gene (subtype C, supplied by Masashi Tatsumi, National Institute of Infectious Diseases), respectively. pUC18 was used as an empty vector.

2.2. Collection of the culture supernatant of viral vector-transfected 293 T cells

Phenol red-free Dulbecco's Modified Eagle Medium (Invitrogen, Rockville, MD), containing 4 mmol/l L-glutamine and 10% fetal calf serum, was used. 293 T cells were plated in a 60 mm dish at 5.0×10^5 cells/ml. pNL4-3, pUC18, pBal, or pIndieC (0.1–8.0 μg) was transfected using Lipofectamine2000 (Invitrogen). At 8 h after transfection, the medium was exchanged with medium containing penicillin (Nacalai Tesque, Kyoto, Japan) and streptomycin (Sigma-Aldrich, St. Louis, MO) as antibiotics. At 48 h, the medium was collected and

* Corresponding author at: Department of Virology, Center for Infectious Disease Control, Research Institute for Microbial Diseases, Osaka University, Yamadaoka 3-1, Suita, Osaka 565-0871, Japan. Tel./fax: +81 6 6879 8309.
E-mail address: sakudo@biken.osaka-u.ac.jp (A. Sakudo).

0009-8981/$ – see front matter © 2011 Elsevier B.V. All rights reserved.
doi:10.1016/j.cca.2011.10.035

centrifuged at 1,500xg and the supernatant was stored at −80 °C until required.

2.3. Ultracentrifugation of culture supernatant

The culture supernatant obtained from the previous section was ultracentrifuged at 100,000×g for 1 h to remove virus particles (L8-55 Ultracentrifuge, rotor type: SW50.1; Beckman Coulter, Brea, CA).

2.4. Measurement of viral production

The amount of HIV-1 p24 in the collected culture supernatant was determined using HIV-1 p24 Antigen-capture enzyme-linked immunosorbent assay (ELISA) (ZeptoMetrix Corp., Buffalo, NY) according to the manufacturer's instructions.

2.5. Western blotting

A 10 μl aliquot of the culture supernatant was suspended in 10 μl of sodium dodecyl sulfate (SDS) sample buffer (50 mmol/l Tris–HCl, pH 6.8, 4% SDS, 12% β-mercaptoethanol, 20% glycerol, 1% bromophenol blue). Proteins in the sample were separated by SDS polyacrylamide gel electrophoresis (PAGE) and then electroblotted onto a polyvinylidene difluoride membrane. The membrane was reacted with serum from a HIV-1-infected patient as a primary antibody and anti-human IgG-HRP as a secondary antibody. Then, reactive bands were detected using enhanced chemiluminescence system (Amersham Biosciences, Uppsala, Sweden). The intensities of two bands of 24 kDa and 55 kDa, which correspond to HIV-1 p24 and p55, respectively, were analyzed using Scion Image 4.03 (Scion Corporation; Frederick, MD).

2.6. NIR spectrum measurement

A 2 ml aliquot of each sample was infused into a polystyrene cuvette for NIRS (SARSTEDT, Numbrecht, Germany) and measurements were performed using a sealed system. Three transmittance spectra of the samples were measured using FQA-NIRGUN (Japan Fantec Research Institute, Shizuoka, Japan) under fixed conditions (37 °C). The NIR spectra were obtained at a 2-nm resolution in the region of 600–1100 nm.

2.7. Principal component analysis (PCA)

NIR spectra were analyzed using Pirouette Version 3.11 (GL Sciences, Inc., Tokyo, Japan). For pretreatment, spectra were normalized using standard normal variate (SNV) and smoothed using 19 data points [17]. In the PCA, wavelength with a larger difference in absorbance was multiplied by a larger factor to increase the dispersion of the dataset [18]. A synthetic variate with the largest dispersion was calculated as the first principal component (PC1), while the one with the second largest dispersion was calculated as the secondary principal component (PC2). Loadings showing the factors of synthetic variates at each wavelength were also calculated.

2.8. Statistical analysis

Statistical analysis was conducted with Student's *t*-test. A p-value<0.05 was considered significant.

3. Results

293 T cells were transfected with pUC18 or pNL4-3 and the culture supernatants were collected 48 h later. The amount of HIV-1 in these culture supernatants was determined by HIV-1 p24 ELISA and Western blotting (Fig. 1). HIV-1 p24 was detected by the HIV-1 p24 ELISA from the culture supernatant of the pNL4-3-transfected 293 T cells, but not from that of pUC18-transfected cells (Fig. 1A). HIV-1 Gag p55 bands were quantified by Western blotting using serum from a HIV-1-infected patient (Fig. 1B). Importantly, the HIV-1 Gag p55 bands were detected from the culture supernatant of pNL4-3-transfected 293 T cells, but not from that of pUC18-transfected cells. Subsequently, NIR spectra were determined for the culture supernatants of pUC18- or pNL4-3-transfected 293 T cells to obtain the original spectra (Fig. 1C and D) and those after pretreatment (SNV + smoothing) (Fig. 1E and F). All the NIR spectra peaked at around 960 nm. The spectra after pretreatment (SNV + smoothing) showed no marked difference in absorption between the culture supernatants of pUC18- or pNL4-3-transfected 293 T cells.

Secondly, the NIR spectra obtained for the culture supernatants of pUC18- or pNL4-3-transfected 293 T cells were pretreated (SNV + smoothing) and subjected to PCA (Fig. 1G, I and J). Fig. 1G shows PCA score plots: pNL4-3-transfected 293 T cells (black diamonds) and pUC18-transfected 293 T cells (white diamonds). The pNL4-3- and pUC18-transfected 293 T cells were divided by the PC1 axis. PC1 loading generated a peak at 950 nm and a minimum at 1030 nm (Fig. 1I). PC2 loading generated peaks at 960 and 630 nm and a minimum at 870 nm (Fig. 1J).

Next, alterations in the NIR spectra after HIV-1 removal by ultracentrifugation were analyzed. 293 T cells were transfected with pNL4-3 and cultured for 48 h. Then, a culture supernatant was collected and ultracentrifuged. The viral load before and after ultracentrifugation were determined by HIV-1 p24 ELISA and Western blotting. The HIV-1 p24 ELISA demonstrated that the amount of virus was reduced to about 10% by ultracentrifugation (Fig. 2A). HIV-1 p55 and p24 bands were quantified by Western blotting and found to be significantly reduced by ultracentrifugation (Fig. 2B and C, respectively). NIR spectra before and after ultracentrifugation were determined 3 times for 3 different culture supernatants. Thus, a total of 9 NIR spectra were obtained. The original NIR spectra (Fig. 2D and E) and NIR spectra after pretreatment (SNV + smoothing) (Fig. 2F and G) were compared for the culture supernatants before and after ultracentrifugation. No marked difference was noted between the two groups. Both groups generated a peak at around 965 nm, presumably resulting from absorption by water molecules in the medium. The NIR spectra after pretreatment (SNV + smoothing) for the culture supernatants before ultracentrifugation and those after ultracentrifugation were subjected to PCA using Pirouette software (Fig. 2H, J, and K). The PCA score plots (Fig. 2H) indicate the culture supernatants before (black diamonds) and after (white diamonds) ultracentrifugation. As shown in Fig. 2H, the culture supernatants before and after ultracentrifugation are clearly divided by the PC1 axis. PC1 loading generated a minimum at 1,034 nm and a peak at 951 nm (Fig. 2J), while PC2 loading generated peaks at 629 and 953 nm and a minimum at 830 nm (Fig. 2K).

Furthermore, nine NIR spectra, obtained from the culture supernatants of the pUC18- or pNL4-3-transfected 293 T cells, were pretreated by SNV + smoothing. Subsequently, the averages of each culture supernatant were calculated to determine difference spectra by subtracting average spectrum for pUC18-transfected 293 T cells from that for pNL4-3-transfected 293 T cells (Fig. 1H). In addition, difference spectra were determined by subtracting average spectra after ultracentrifugation from those before ultracentrifugation (Fig. 2I). Both of these difference spectra showed a peak at around 950 and a minimum at around 1030 nm, which corresponded to PC1 loading by PCA (Figs. 1I and 2J).

Finally, the culture supernatants of cells transfected with various HIV-1 subtype molecular clone vectors were compared. Culture supernatants were obtained 48 h after 293 T cells were transfected with either a subtype B molecular clone, pNL4-3 or pBal, or a subtype C molecular clone, pIndieC (8, 4, 1 and 0.1 μg, respectively) or pUC18 (8 μg). As a further control, untreated 293 T cells and cells treated with Lipofectamine 2000 were also analyzed. The amount of virus in these culture supernatants was determined by HIV-1 p24 ELISA (Fig. 3A) and Western blotting of HIV-1 p55 (Fig. 3B). Both ELISA

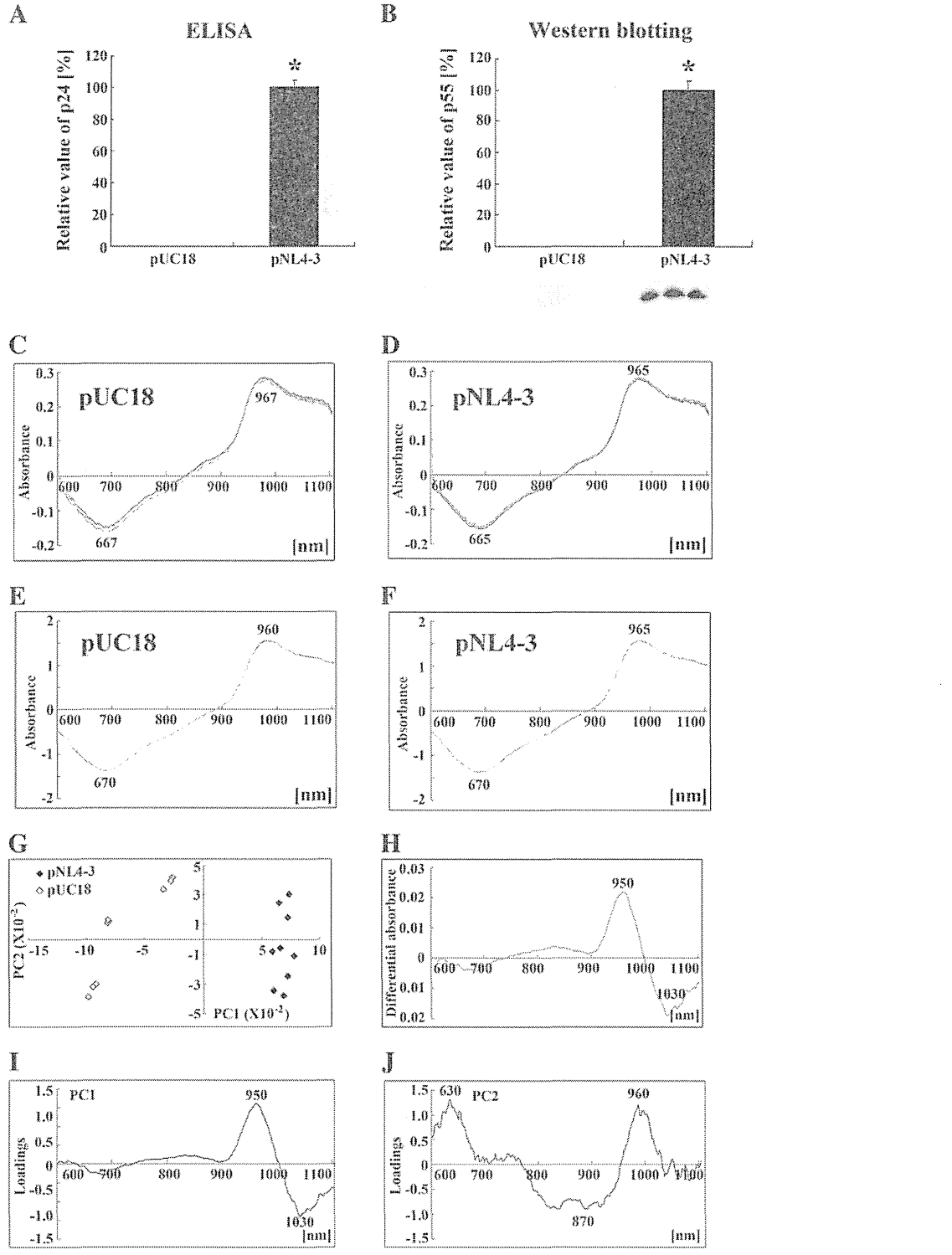

Fig. 1. Detection of HIV-1-related NIR spectra by transfection with an HIV-1 molecular clone. (A–B) Culture supernatants were collected after 48-h of growth of pUC18- or pNL4-3-transfected 293 T cells. The amount of HIV-1 in the culture supernatants was compared by HIV-1 p24 ELISA (A) and Western blotting of HIV-1 p55 (B) ($N=3$). The lower panel shows the bands of interest. The upper panel shows a comparison of band intensities using Scion Image 4.03 (Scion Corporation). An asterisk denotes a significant difference of pNL4-3-transfected 293 T cells compared to pUC18-transfected 293 T cells ($p<0.05$). (C–F) NIR spectra obtained using the culture supernatants collected after 48-h growth of pUC18- or pNL4-3-transfected 293 T cells. The original NIR spectra for pUC18 (C) and pNL4-3 (D) are shown. (E) and (F) show NIR spectra after pretreatment (SNV + smoothing) of (C) and (D), respectively. Each measurement was repeated 3 times using 3 different samples. (G, I, J) The NIR spectra obtained using the culture supernatants collected after 48-h of growth of pUC18- or pNL4-3-transfected 293 T cells were subjected to PCA. (G) In the PCA score plots, black diamonds indicate the culture supernatants of pNL4-3-transfected 293 T cells, whereas white diamonds indicate the culture supernatants of pUC18-transfected 293 T cells. (H) Difference spectra obtained by subtracting average NIR spectra for pUC18-transfected 293 T cells from those for pNL4-3-transfected 293 T cells after pretreatment at each wavelength. (I) and (J) show PC1 and PC2 loadings in the PCA, respectively.

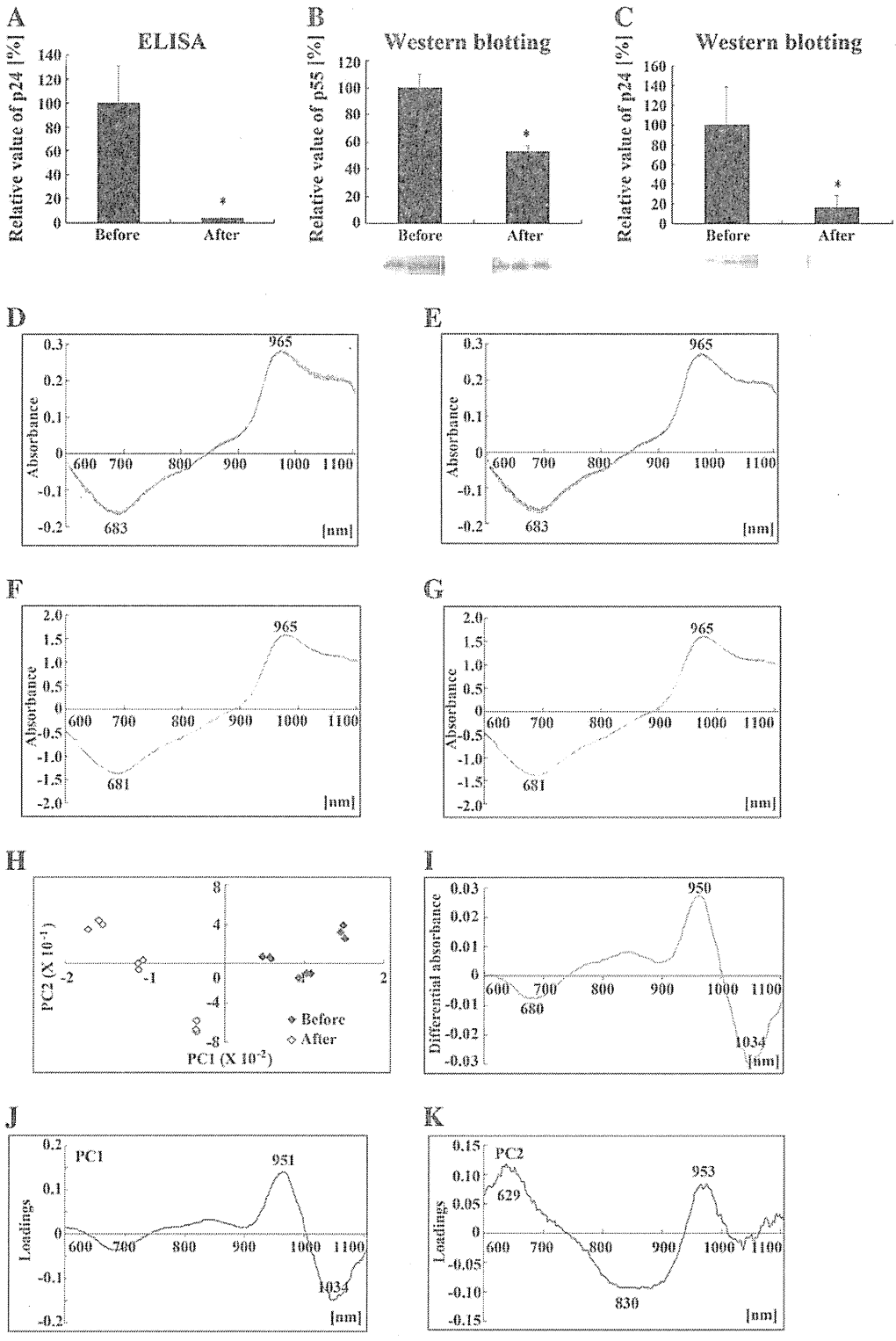

Fig. 2. Effects of HIV-1 removal by ultracentrifugation on NIR spectra. (A–C) The amount of HIV-1 component proteins in the supernatants of HIV-1-infected cells before and after ultracentrifugation was compared. 293 T cells were transfected with pNL4-3 and cultured for 48 h before collecting the culture supernatant. The amount of HIV-1 was compared by HIV-1 p24 ELISA (A) and Western blotting of HIV-1 p55 (B) and p24 (C) ($N=3$). The lower panel shows a Western blot (B) and (C) of the bands of interest. The upper panel shows a comparison of band intensities using Scion Image 4.03 (Scion Corporation). An asterisk denotes a significant difference of the culture supernatants after ultracentrifugation compared to those before ultracentrifugation ($p<0.05$). (D–G) NIR spectra were obtained using the culture supernatants collected from pNL4-3-transfected 293 T cells before and after ultracentrifugation. Original NIR spectra before ultracentrifugation (D) and after ultracentrifugation (E) are shown. (F) and (G) show NIR spectra after pretreatment (SNV + smoothing) of (D) and (E), respectively. Each measurement was repeated 3 times for 3 different samples. (H, J, K) NIR spectra for culture supernatants before and after ultracentrifugation were subjected to PCA. (H) PCA score plots showing the culture supernatants before ultracentrifugation (black diamonds) and after ultracentrifugation (white diamonds). PC1 (J) and PC2 (K) loadings in the PCA are shown. (I) Difference spectra were obtained by subtracting average NIR spectra after ultracentrifugation from those after pretreatment and before ultracentrifugation at each wavelength.

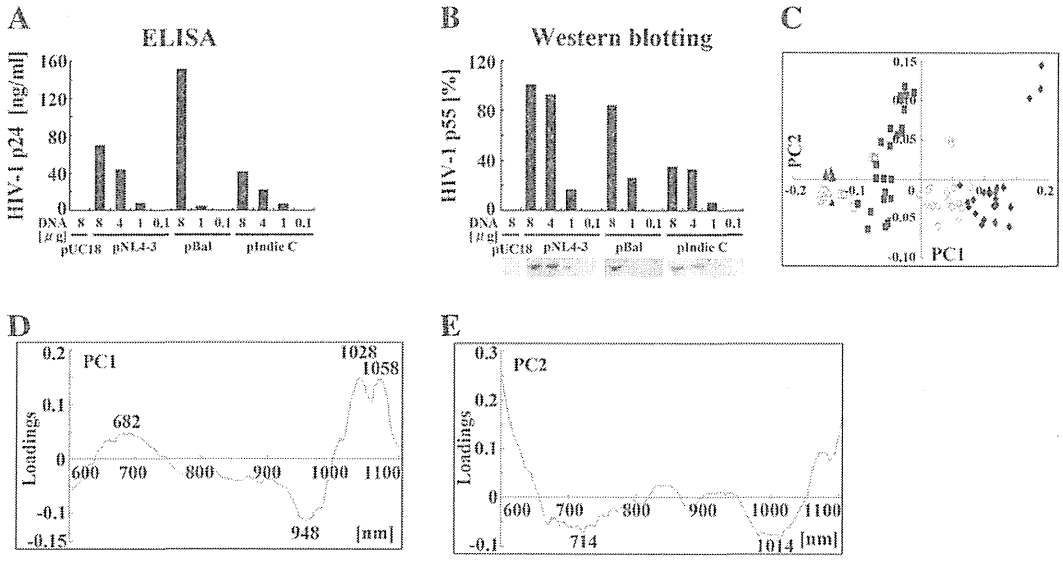

Fig. 3. Detection of HIV-1-related NIR spectra by transfection with HIV-1 subtype B and C molecular clones. The amount of HIV-1 was compared by HIV-1 p24 ELISA (A) and Western blotting of HIV-1 p55 (B). The lower panel shows the bands of interest. The upper panel shows a comparison of band intensities using Scion Image 4.03 (Scion Corporation). (C–E) NIR spectra obtained for culture supernatants of pUC18-, pNL4-3-, pBal- and pIndieC-transfected 293 T cells (48-h growth) after being subjected to PCA. (C) PCA score plots of the NIR spectra were obtained for culture supernatants of pUC18- (white square), pNL4-3- (black diamond), pBal- (white diamond), and pIndieC- (black square) transfected 293 T cells as well as medium alone (non-treatment) (white triangle) and lipofectamine2000-containing medium (black triangle). PC1 (D) and PC2 (E) loadings in the PCA are shown.

and Western blotting demonstrated the presence of HIV-1 in the culture supernatants of pNL4-3-, pBal-, or pIndieC-transfected cells. NIR spectra were determined three times for three culture supernatants. NIR spectra after pretreatment (SNV + smoothing) were subjected to PCA (Fig. 3C–E). The PCA score spots (Fig. 3C) demonstrated that subtype B (pNL4-3 and pBal) and subtype C (pIndieC) were divided by the PC1 axis. The culture supernatants of pUC18-transfected, Lipofectamine 2000-transfected, and untreated cells were classified into almost identical groups. The PCA showed that PC1 loading generated peaks at 1028 and 1058 nm and a minimum at 948 nm (Fig. 3D), while PC2 loading generated minima at 714 and 1014 nm (Fig. 3E).

4. Discussion

Herein, we describe a novel approach utilizing NIRS that can be used to differentiate cells transfected with various HIV-1 molecular cloning vectors. In all our experiments, NIR spectra showed an absorption peak at around 950 nm, which appears to be caused by the combination tone of OH vibration in water [9]. Initially, no marked differences were observed in the presence or absence of HIV-1. However, we subsequently showed that NIR spectra can be subtracted to reveal characteristic absorbance differences. Difference NIR spectra after pretreatment (SNV + smoothing) were obtained by subtracting the average NIR spectra after ultracentrifugation from those before ultracentrifugation. Using these difference spectra, supernatants with a larger amount of HIV-1 (i.e., before ultracentrifugation) displayed an absorption minimum at around 1,030 nm and an absorption peak at around 950 nm as compared with supernatants with a reduced amount of HIV-1 (i.e., after ultracentrifugation). In addition, difference NIR spectra, obtained by subtracting the average NIR spectra for the culture supernatant of pNL4-3-transfected 293 T cells from those for the culture supernatant of pUC18-transfected 293 T cells were also obtained. The difference spectra of samples with HIV-1 had an absorption minimum at around 1,030 nm and an absorption peak at around 950 nm as compared with those without HIV-1. The PC1 loadings were comparable among all the experiments. Thus, the absorbance at around 950 and 1030 nm are related to the presence or absence of HIV-1 and to changes in the amount of HIV-1 in the sample. These findings are largely consistent with a previous report using HIV-1 infected plasma, which employed partial least squares regression (PLS) to establish the most suitable wavelength for quantifying HIV-1 [10]. This previous analysis, which covered 600–1000 nm, showed that 954 nm was the most appropriate wavelength for measuring the level of HIV-1. In addition, 686 and 802 nm made a minor contribution to quantifying the amount of virus. Therefore, with the exception of the peak at 686 nm, the majority of peaks analyzed between the two reports are common. A difference of sample type, such as cell culture medium and plasma, could account for this minor variation in the data analysis.

A comparison of the samples before and after ultracentrifugation suggests that the culture supernatants differ because of various factors, such as precipitates (other than HIV-1) after ultracentrifugation. In the pNL4-3 transfection experiment, cellular alterations caused by HIV-1 infection (e.g., cytokine secretion) may have changed the culture supernatant components. In addition, there is a possibility of producing heterogeneous viruses dependent on host cells. However, the constituents of the medium and heterogeneity of the virus do not appear to critically affect NIR spectra. Indeed, the current study using cell culture medium of 293 T cells for HIV-1 showed an important absorption at around 950 nm, which is similar to the previous result using HIV-1 infected plasma (with the exception of the peak at 686 nm) [10]. The experiment with subtype B and C molecular clones suggested that various HIV-1 subtypes could be identified. Specifically, the HIV-1 subtypes can be differentiated and identified by the NIR spectra i.e., HIV-1-infected culture supernatants can be divided into subtypes by analyzing the absorption at around 682, 948, 1028 and 1058 nm, which are important wavelengths for discrimination of subtype B and C (Fig. 3D). As shown for the PCA loadings before and after ultracentrifugation and in the presence and absence of HIV-1, PC1 loadings with transfection of various HIV-1 subtype molecular clone vectors showed peaks at around 950, 1030, and 1060 nm. PCA score plots became comparable with those of HIV-1-free culture supernatants (Lipofectamine2000-added and untreated cell media) as the amount of HIV-1 molecular clone vector to be transfected was decreased. Hence, NIR spectra can be used to evaluate the amount of HIV-1 present in the sample. These findings indicate the presence of HIV-1 can be detected by characteristic features of the spectra at 950, 1030, and 1060 nm.

OH absorption occurs in the region of 600–1100 nm. Specifically, if v_1 is the symmetric stretching vibration of OH and v_2 is the asymmetric

stretching vibration of O—H, the absorption of combination tone ($2\nu_1 + \nu_2$) occurs at around 950 nm [9]. Thus, HIV-1 may have altered the absorption of the above combination tone of OH. This suggests that HIV-1 interacts with water in the medium and the interaction occurs as NIR absorptions at around 950, 1030, and 1060 nm. Thus, NIRS may be useful in analyzing the interaction between water and HIV-1. As far as we know, NIRS is the only tool to analyze the interaction between virus and water. How the interaction between HIV-1 and water varies among different HIV-1 subtypes is intriguing. In addition, it remains unclear whether NIRS can discriminate between HIV-1 and HIV-2; HIV-1 groups (M, O, and N); HIV-1 subtypes (A to J) besides subtype B and C; and even circulating recombinant forms of virus [19].

In summary, we transfected 293 T cells with an HIV-1 molecular clone, pNL4-3, and collected the culture supernatant. We subsequently employed NIRS to compare culture supernatants with viruses either before or after ultracentrifugation of the sample. Supernatants of cells transfected with pUC18 (empty vector for pNL4-3), and those of cells transfected with various HIV-1 subtype molecular clone vectors were also analyzed. PCA and examination of the difference spectra demonstrated that NIRS can be used to study the interaction between HIV-1 and water. The interaction showed different characteristics among HIV-1 subtypes. These findings suggest that difference of NIR spectra caused by interaction with water among HIV-1 subtypes may enable the discrimination of HIV-1 subtypes spectroscopically.

Acknowledgements

This study was supported in part by the Japan Science and Technology Agency, the Ministry of Education, Culture, Sports, Science and Technology (MEXT) of Japan.

References

[1] Diem M, Griffiths PR, Chalmers JM. Vibrational Spectroscopy for Medical Diagnosis. Chichester: John Wiley & Sons Ltd.; 2008.
[2] Lasch P, Kneipp J. Biomedical vibrational spectroscopy. Chichester: John Wiley & Sons Ltd.; 2008.
[3] Shaw RA, Kotowich S, Mantsch HH, Leroux M. Quantitation of protein, creatinine, and urea in urine by near-infrared spectroscopy. Clin Biochem 1996;29:11–9.
[4] Sakudo A, Tsenkova R, Tei K, Onozuka T, Ikuta K, Yoshimura E, Onodera T. Comparison of the vibration mode of metals in HNO_3 by a partial least-squares regression analysis of near-infrared spectra. Biosci Biotechnol Biochem 2006;70: 1578–83.
[5] Sakudo A, Yoshimura E, Tsenkova R, Ikuta K, Onodera T. Native state of metals in non-digested tissues by partial least squares regression analysis of visible and near-infrared spectra. J Toxicol Sci 2007;32:135–41.
[6] Kobayashi T, Kato YH, Tsukamoto M, Ikuta K, Sakudo A. Portable visible and near-infrared spectrophotometer for triglyceride measurements. Int J Mol Med 2009;23:75–9.
[7] Tsenkova R. Introduction aquaphotomics: dynamic spectroscopy of aqueous and biological systems describes peculiarities of water. J Near Infrared Spectrosc 2009;17:303–13.
[8] Sakudo A, Suganuma Y, Kobayashi T, Onodera T, Ikuta K. Near-infrared spectroscopy: promising diagnostic tool for viral infections. Biochem Biophys Res Commun 2006;341:279–84.
[9] Workman Jr J, Weyer L. Practical guide to interpretive near-infrared spectroscopy. New York: CRC Press; 2008.
[10] Sakudo A, Tsenkova R, Onozuka T, Morita K, Li S, Warachit J, Iwabu Y, Li G, Onodera T, Ikuta K. A novel diagnostic method for human immunodeficiency virus type-1 in plasma by near-infrared spectroscopy. Microbiol Immunol 2005;49:695–701.
[11] Bahmani MK, Khosravi A, Miri R, Iwabu Y, Ikuta K, Sakudo A. Spectroscopic characterization of human immunodeficiency virus type-1-infected plasma by principal component analysis and soft independent modeling of class analogy of visible and near-infrared spectra. Mol Med Report 2009;2:805–9.
[12] H. Xu, S. Zhu, Y. Ying, H. Jiang, Application of multispectral reflectance for early detection of tomato disease. In Proceedings of the Society of Photo-Optical Instrumentation Engineers: 3–4 October 2006; Boston. Edited by the Society of Photo-Optical Instrumentation Engineers. Bellingham: ETATS-UNIS; 2006:63810R.1-63810R.8.
[13] Jinendra B, Tamaki K, Kuroki S, Vassileva M, Yoshida S, Tsenkova R. Near infrared spectroscopy and aquaphotomics: novel approach for rapid in vivo diagnosis of virus infected soybean. Biochem Biophys Res Commun 2010;397:685–90.
[14] Petisco C, Garcia-Criado B, Zabalgogeazcoa I, Vázquez-de-Aldana BR, Garcia-Ciudad A. A spectroscopy approach to the study of virus infection in the endophytic fungus *Epichloë festucae*. Virol J 2011;8:286.
[15] Adachi A, Gendelman HE, Koenig S, Folks T, Willey R, Rabson A, Martin MA. Production of acquired immunodeficiency syndrome-associated retrovirus in human and nonhuman cells transfected with an infectious molecular clone. J Virol 1986;59:284–91.
[16] Mochizuki N, Otsuka N, Matsuo K, Shiino T, Kojima A, Kurata T, Sakai K, Yamamoto N, Isomura S, Dhole TN, Takebe Y, Matsuda M, Tatsumi M. An infectious DNA clone of HIV type 1 subtype C. AIDS Res Hum Retroviruses 1999;15:1321–4.
[17] Savitzky A, Golay MJE. Smoothing and differentiation of data by simplified least-squares procedures. Anal Chem 1964;36:1627–39.
[18] Miller JN, Miller JC. Statistics and chemometrics for analytical chemistry. UK: Prentice Hall College Div; 2000.
[19] Murray PR, Baron EJ, Pfaller MA, Tenover FC, Yolken RH. Manual of clinical microbiology. 7th ed. Washington: ASM Press; 2001.

Dengue virus presence and surveillance in Okinawa (Review)

AKIKAZU SAKUDO[1], TAKASHI ONODERA[2], HIDEHARU SHINTANI[3] and KAZUYOSHI IKUTA[4]

[1]Laboratory of Biometabolic Chemistry, School of Health Sciences, Faculty of Medicine, University of the Ryukyus, Okinawa 903-0215; [2]Research Center for Food Safety, Graduate School of Agricultural and Life Sciences, The University of Tokyo, Tokyo; [3]Faculty of Science and Engineering, Chuo University, Tokyo 112-8551; [4]Department of Virology, Center for Infectious Disease Control, Research Institute for Microbial Diseases, Osaka University, Osaka 565-0871, Japan

Received August 25, 2011; Accepted September 9, 2011

DOI: 10.3892/etm.2011.371

Abstract. Recent reports have shown that the dengue virus (DENV) is a serious concern worldwide, especially in subtropical areas such as South-East Asia. With the development of transportation systems, the risk of DENV infection spreading is increasing. Since mosquitoes transmit DENV to humans, surveillance of DENV-infected mosquito vectors is the most effective approach for preventing DENV. Okinawa is the only prefecture located in a subtropical region in Japan and historically shows continuous importation of DENV-related mosquito vectors. In this review, we describe the current and historical status of DENV in Okinawa.

Contents

1. Introduction

A plus-strand RNA virus, the dengue virus (DENV), can be transmitted through mosquito vectors, and these infections lead to dengue fever (DF), dengue hemorrhagic fever (DHF) and dengue shock syndrome (DSS) (1). DHF and DSS are potentially lethal. The risk of developing them is correlated with infection by one of the four DENV serotypes (DENV1 to DENV4) and having antibodies to another DENV serotype from a previous infection (2). Currently, no specific treatment or vaccine for DENV is available (3).

Recently, reports that DENV has rapidly spread and infected or killed humans have increased (1). In the last 50 years, the incidence has increased by 30-fold. Infection of DENV is estimated at 50 million cases annually (WHO). Among these, Asia and the Pacific region constitute 75% of the current global disease burden (3). As DENV spreads beyond national borders, the emergence of DENV is of particular concern to public health. In this review, we report the current and past conditions of dengue disease in Okinawa.

2. History of dengue disease in Okinawa and Japan

Okinawa is the southwestern-most prefecture in Japan and consists of a chain of hundreds of islands in the Ryukyu Archipelago, which is over 1,000 km long (Fig. 1). The location is approximately half-way between Kyushu (the southwest region of Japan's main four islands) and Taiwan. The first reports of dengue disease in Japan were in 1893 and 1903 (4) (Table I). Although the case in 1893 was not diagnosed as dengue disease, the invasion route, epidemic status and disease condition suggest that it was DF. In 1903, Dr Jiro Kawamura diagnosed DF in the Yaeyama Islands. This is thought to be the start of the DF epidemic in Japan (5). Although fever epidemics were frequently found after 1893, that of DF was only found in 1893 and 1904 in the Meiji era (1868-1912). At that time, DF showed weak symptoms and caused a low incidence of death. In addition, severe diseases such as cholera and smallpox hid the DF condition.

In July 1903, DF was first diagnosed in the Yaeyama Islands. Subsequently, DF spread to the Miyako Island and the Okinawa main island in September and October, respectively (6). In 1904, DF was still prevalent in Yaeyama and Miyako Islands and the Okinawa main island, and resulted in 61,901 patients and 16 deaths (7,8).

In the Taisho era (1912-1926), the incidence of DF decreased compared to the Meiji era, whereas in 1916 and 1924 DF epidemics were reported (9,10). In the Showa era (1926-1989), DF incidence was found in Japan in 1931, 1934, 1942, 1943 and 1944, whereas there were no incidences after World War II (1939-1945). In Okinawa, a major outbreak of DF was found on Ishigaki Island in 1930. Then, DF spread to the Miyako Island,

Correspondence to: Dr Akikazu Sakudo, Laboratory of Biometabolic Chemistry, School of Health Sciences, Faculty of Medicine, University of the Ryukyus, 207 Uehara, Nishihara, Okinawa 903-0215, Japan
E-mail: sakudo@med.u-ryukyu.ac.jp

Key words: dengue, mosquito, Okinawa, Ryukyu, Taiwan

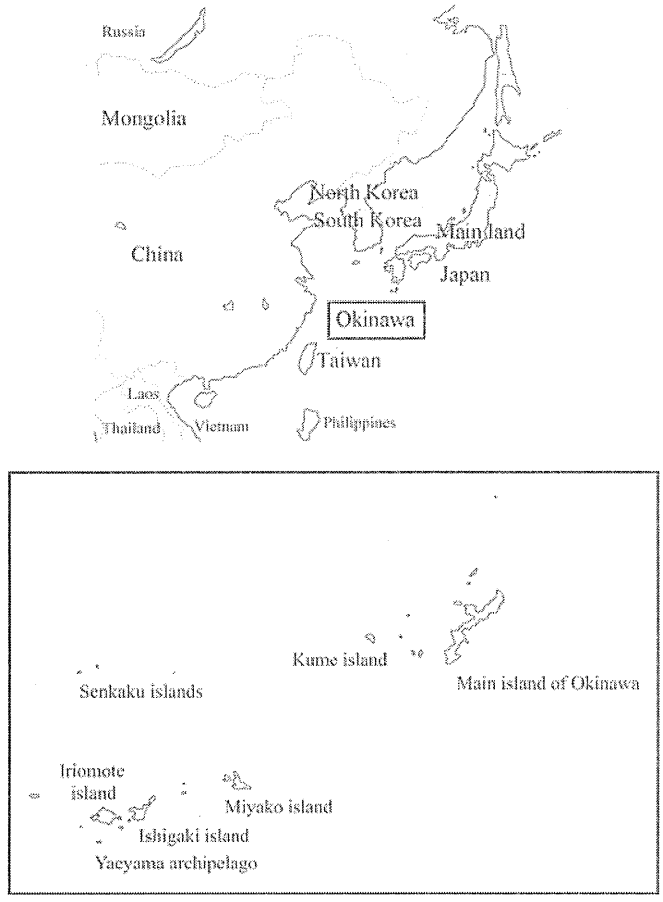

Figure 1. Location of the Okinawa prefecture and Taiwan. Okinawa prefecture is located in the southwest region of Japan. An enlarged illustration of Okinawa Islands is shown in the box.

the Okinawa main island and Kagoshima prefecture on the mainland of Japan (11). After World War II, DF incidence was not found on the main island of Okinawa or the mainland of Japan (12).

In general, the most common invasion route of DF into Okinawa was through the Yaeyama Islands. Then, DF reached the Naha port on the Okinawa main island via the Miyako Island. From Naha, DF spread to other regions of the Okinawa main island and the surrounding islands (13). Therefore, it is reasonable to suggest that most DENV incidents in Okinawa originated from Taiwan, especially in light of mercantile routes of ships during this time. In addition, although *Aedes aegypti* was previously detected, none was detected after the 1970s in Japan. By contrast, in southern Taiwan, *Aedes aegyptia* was prevalent. As Taiwan is very close to Okinawa, the continued surveillance for DENV invasion from Taiwan via airplanes and ships is important. Evaluating the distribution of mosquito vectors in this broad region will be useful for the efficient prevention of the appearance and growth of mosquitoes by using chemicals or other methods.

3. Recent condition of dengue disease in Okinawa and the surrounding region

Two DENV mosquito vectors (*Aedes aegypti* and *Aedes albopictus*) were found during the epidemics in the early

Table I. History of major DF epidemics in Okinawa and Japan (4).

Cases	All Japan	Okinawa
1	1893	1893
2	1902	1904
3	1912	1915
4	1916	1931
5	1924	
6	1931	
7	1934	

20th century in Okinawa and on mainland Japan (14-17). It should be noted that mosquitoes' eggs remain viable for over a year in dry conditions, while the eggs are deposited in the presence of water (3). This allows the mosquito to re-emerge after a cold winter or dry spell. Previous studies have shown that peak mosquito generation was found in the summer season in a pig livestock barn on Yonaguni Island and a public park in Naha City (18). Therefore, close attention should be paid to the mosquito status during the summer season when invasion of DENV is detected in Okinawa or the surrounding region.

An outbreak of DENV3 occurred in southern Taiwan in 1998 (3,19) and, in 2002, more than 15,000 individuals were infected with DENV in Taiwan. In addition, major dengue outbreaks in Taiwan have been reported (20). Taiwan is located 110 km from Yonaguni Island, which is the last of the Ryukyu Islands chain and the western-most inhabited island of Japan. In epidemiological studies, a wide variety of DENV strains were isolated from imported and indigenous dengue cases during the outbreak of 1981-2006 in Taiwan (20). The results of molecular epidemiology suggested that constant importation of multiple DENVs via mosquitos and individuals from neighboring southeast Asian countries through close commercial links and air travel was responsible for local outbreaks. In Japan, quarantine stations at airports and harbours have performed surveillance for DENV-infected mosquitoes. However, in Okinawa there are US military bases, which the Japanese government cannot control. Therefore, there is the possibility that DENV-infected mosquitoes may invade Okinawa via military airplanes or ships. In addition, the monitoring of migratory wildfowl is necessary, as many birds come to Okinawa in the spring and autumn. In particular, surveillance on Yonaguni Island is important.

Although there are four distinct serotypes (DENV1 to DENV4), molecular analysis during 2003-2007 showed that the geographic distribution of DENV3 strains and genotypes isolated from southeast Asian countries remained unchanged during 2003-2007, whereas the movement and establishment of new DENV1, DENV2 and DENV4 strains were observed in certain areas of Asia (21). Among them, DENV2 and DENV3 genotypes are frequently associated with severe disease accompanying secondary infection, known as antibody-dependent enhancement (2). Therefore, distribution of DENV-infected mosquitoes, especially DENV2 and DENV3, should be observed closely. Thus, effective and sensitive methods for detecting DENV in mosquitoes are required.

4. Conclusion

Herein, we reviewed the current and past presence of DENV incidence in Okinawa and presented a personal view regarding the future perspectives. During 1838-1955, epidemics of dengue disease were reported 10-20 times in Okinawa. Currently, the incidence of DENV infection has not been reported in Okinawa, and DENV-infected mosquitoes are not resident there. However, several (more than 10) incidences of imported infection cases have been reported annually (22). To prepare for the invasion of DENV, the investigation of resident and generated mosquito vectors in surrounding circumstances should be performed. Although, currently, vector surveillance has focused on airports and harbours, the conditions of public parks, livestock barns and stopovers for migratory birds should be also checked.

Acknowledgements

This study was supported in part by the Japan Science and Technology Agency and the Ministry of Education, Culture, Sports, Science and Technology (MEXT) of Japan.

References

1. World Health Organization: http://www.who.int/mediacentre/factsheets/fs117/en/ (Accessed May 20, 2011).
2. Morens DM: Antibody-dependent enhancement of infection and the pathogenesis of viral disease. Clin Infect Dis 19: 500-512, 1994.
3. World Health Organization: Dengue Hemorrhagic Fever, Diagnosis, Treatment and Control. 2nd edition. World Health Organization, Geneva, 1997.
4. Inafuku S: The History of Diseases in Okinawa. Daiichi Shobo Co., Ltd., Tokyo, 1995.
5. Ryukyu Shimpo Newspaper. October 1, 5, 7, 27, 1903.
6. Ryukyu Shimpo Newspaper. October 1, 17, 27, 1903.
7. Government of the Ryukyu Islands: Okinawan History. Vol. 19, 1969.
8. Editorial Committee of History of Taira City: History of Taira City, 1985.
9. Takaka K: Gynecological symptoms of Dengue fever in Okinawa Prefecture in Taisho 4. Reports of Okinawa Medical Association, Okinawa, No. 43, 359-378, 1917.
10. Health and Medical Division, Okinawa Prefecture: Outline of Hygiene in Okinawa, pp63-85, 1924.
11. Yoshino T: Dengue fever in Southern Okinawa. Jpn J Clin Exp Med 20: 943, 1943.
12. The Okinawa Times. April 8, 1960.
13. Ura M: Epidemiology of Dengue Fever in Okinawa. Annual Report of Okinawa Prefectural Institute of Public Health, No. 12, 1978.
14. Hawley W: The biology of *Aedes albopictus*. J Am Mosq Control Assoc 1: S1-S39, 1988.
15. Gubler DJ and Kuno G: Dengue and Dengue Hemorrhagic Fever. CAB International Publishing, New York, 1997.
16. Gratz NG: Critical review of the vector status of *Aedes albopictus*. Med Vet Entomol 18: 215-227, 2004.
17. Hotta S: Dengue vector mosquitoes in Japan: the role of *Aedes albopictus* and *Aedes aegypti* in the 1942-44 dengue epidemics of Japanese main islands. Med Entomol Zool 49: 276-284, 1998.
18. Taira K, Itokzu K, Kudaka J, Nidaira M, Ohno A and Nakamura M: A survey of mosquitoes as Flavivirus vector in Okinawa prefecture. Annual report of Okinawa Prefectural Institute of Health and Environment 41: 39-44, 2007.
19. Harris E and Roberts G: Typing of dengue viruses in clinical specimens and mosquitoes by single-tube multiplex reverse transcriptase PCR. J Clin Microbiol 36: 2634-2639, 1998.
20. Huang JH and Liao TL: Laboratory-based dengue surveillance in Taiwan, 2005: a molecular epidemiologic study. Am J Trop Med Hyg 77: 903-909, 2007.
21. Shu PY and Su CL: Molecular characterization of dengue viruses imported into Taiwan during 2003-2007: geographic distribution and genotype shift. Am J Trop Med Hyg 80: 1039-1046, 2009.
22. Infectious Disease Surveillance Center: Infectious Agents Surveillance Report. Vol. 25, pp1-2, 2004.

FULL PAPER *Virology*

The Influence of Borna Disease Viral Infection on Dairy Cow Reproduction

Katsuro HAGIWARA[1)]*, Tatsuya ANDO[2)] and Masateru KOIWA[1)]

[1)]*School of Veterinary Medicine, Rakuno Gakuen University, Ebetsu, Hokkaido 069–8501, Japan*
[2)]*Ishikari Agricultural Mutual Relief Association, Hokkaido 067–0055, Japan*

(Received 27 July 2011/Accepted 11 November 2011/Published online in J-STAGE 25 November 2011)

ABSTRACT. We investigated the influence of Borna disease virus (BDV) infection on the clinical state of dairy cows. Sera from 149 cows were examined using enzyme-linked immunosorbent assay and western blotting detect antibodies to the BDV-nucleoprotein antigen. Among 149 investigated cows, 25 (16.8%) showed a positive reaction to BDV antigen. No significant difference existed in milk production or medical history between seropositive and seronegative cows. Although the estrus cycle appeared normal even in the seropositive cows, the frequency of artificial insemination and calving-to-conception intervals significantly increased in seropositive cows. Therefore, fertilization failure was recognized in the BDV-antibody positive cows.
KEY WORDS: borna disease virus, cow, sterility.

doi: 10.1292/jvms.11-0356; *J. Vet. Med. Sci.* 74(4): 419–421, 2012

Borna disease virus (BDV) is the causative agent of Borna Disease (BD), an immune-mediated neurological disease first described in horses, more than 200 years ago in southern Germany [11, 17, 18]. Initially, BD was thought to be restricted to horses and sheep in central Europe; subsequent epidemiological evidence has indicated that the prevalence and geographic distribution, as well as the host range of BDV, are broader than previously thought [16–18].

Epidemiological studies have documented the presence of serum antibodies to BDV and virus RNA in the brains of domestic animals and companion animals in several countries, including Japan [3, 5, 8, 14, 19]. Recently, BDV-infected dogs, cats, macaques, and raccoons have been reported in Japan [6, 10, 13, 15]. Dairy cows with BDV infection are recognized as seropositive individuals, although the infections are latent, and the cows never show any neurological symptoms. Conversely, studies regarding the prevalence of disease in BDV-antibody positive racehorses indicate that BDV infection may possibly contribute to an increase in the incidence rate of locomotion disorders in racehorses [9].

To investigate the prevalence of disease in BDV-antibody positive dairy cows on a farm, that have had Borna disease in the past, we conducted seroepidemiological studies and observed the clinical symptoms of 149 dairy cows in Hokkaido, Japan.

MATERIALS AND METHODS

Serological analysis: A total of 149 Holstein dairy cows (107 multiparous cows, 42 heifers) were examined for serological analysis to BDV antigen. The examined cows were born and reared at the same farm where a BDV-positive cow was confirmed in the past [14]. Serum samples were diluted at 1:100 with phosphate buffered saline containing 10% Block Ace (Dainippon Pharmaceutical Co., Osaka, Japan) and 0.05% Tween 20 and screened for antibodies to BDV by ELISA using the recombinant BDV nucleoprotein (BDV-N) antigen as described in our previous reports [4, 9]. To detect antigen-bound bovine immunoglobulin, a peroxidase-conjugated goat affinity purified anti-bovine IgG (Bethyl Laboratories, Inc., Montgomery, TX, U.S.A.) was used; positive reactions were identified using Microplate Imaging System (Ultramark, Bio-Rad, Hercules, Contra Costa, CA, U.S.A.) at 405 nm. The cutoff value for ELISA was calculated as the mean ± 2SD at OD of 405 nm of 5 intact cows (cutoff: OD, 0.4). ELISA-positive samples were further examined by western blotting using recombinant BDV-N as the target antigen. Antibody-antigen complexes were detected using the same peroxidase-conjugated goat affinity purified anti-bovine IgG mentioned above, as described elsewhere [5, 12].

Clinical records: The clinical records of cows were checked for 2 years before serological examination was conducted for quantity and quality of milk production, clinical disease history, and breeding history. The clinical records of the cows were investigated for the following conditions: dysfunction of locomotion (DL); dysfunction of the nervous system (DN), including cryptogenic behavioral changes with paralysis; and dysfunction of the alimentary systems (DA), including severe colic, penetration of the intestine, and peritonitis. The incidence and the factors related to the breeding conditions were determined on the basis of the following measures: lactation number, frequency of artificial insemination (AI), non-pregnant terms (the calving-to-conception intervals), and parturition season. Statistical analysis of disease incidence and seroprevalence were calculated using the chi-square test for independence.

*CORRESPONDENCE TO: HAGIWARA, K., School of Veterinary Medicine, Rakuno Gakuen University, Ebetsu, Hokkaido 069–8501, Japan.
e-mail: k-hagi@rakuno.ac.jp

Table 1. Summary of reproduction score and milk production data in seropositive cows

Multiparous cows Cow number	Non-pregnant terms (month)	AI	Number of births	Milk production	Milk Fat (%)	Milk Protein (%)
391	11.4	1	8	10900	4.2	3.0
416	14.0	3	7	9550	4.3	3.1
422	12.6	1	6	10885	4.9	3.3
458	14.3	4	5	10400	4.5	3.2
460	10.7	1	6	NA	NA	NA
481	14.6	1	5	8900	4.0	2.9
483	15.4	2	4	9700	4.3	3.3
501	24.2	9	2	12775	3.7	3.0
502	17.5	5	3	13200	3.8	3.0
503	12.6	2	3	9511	4.2	3.3
507	15.7	6	3	11000	4.2	3.0
543	15.0	4	2	12700	3.9	3.0
549	23.0	11	1	12637	4.2	3.2
551	24.6	10	1	11272	3.8	3.1
556	17.0	4	2	11700	3.4	3.0
558	20.9	9	1	12252	3.9	3.1
562	13.3	1	1	10028	4.5	3.3
567	11.6	1	1	12424	3.4	3.1
575	17.0	4	1	12300	3.6	2.9
576	14.1	3	1	10100	4.1	2.9
Heifers	First calving age	AI	Number of births	Milk production	Milk Fat	Milk Protein
629	29.9	5	0	–	–	–
668	27.3	2	0	–	–	–
669	29.7	5	0	–	–	–
702	26.8	4	0	–	–	–
703	23.2	1	0	–	–	–

AI: frequency of artificial insemination, NA: Data not available.

RESULTS

Our serological study indicated that 20 of 107 multiparous cows (18.7%) were diagnosed as seropositive cows. Among the heifers, 5 of 42 (11.9%) were seropositive. A total of 25 cows (16.8%) were seropositive for BDV. The average number of births was 3.4 in the seronegative group and 3.2 in the seropositive group. The clinical history showed that there was no significant difference in the clinical records (DL, DA, etc.) between the seropositive and seronegative cows. Clinical investigations showed the presence of neuroticism, hypodynamia, and dysstasia in some of the seropositive cows; however, this difference between the seropositive and seronegative cows was not statistically significant. No significant difference in the quantity and quality of milk production was observed between the groups. The average milk produced per milking period was 10,610 kg (seronegative) and 11,170 kg (seropositive). After investigation of the breeding condition, all the cows were found to be clinically normal; however, fertilization failure was observed in the seropositive cows. In multiparous cows, the frequency of AI increased significantly in the seropositive cows (average, 4.1) and prolonged non-pregnant terms (average, 16.0 months) as compared to the seronegative cows. Half of the antibody-positive cow enforced AI more than four times. The frequencies of AI and non-pregnant terms were 2.1 times and 13.5 months in seronegative cows, respectively (Tables 1 and 2, $P<0.05$). Interestingly, a similar phenomenon was observed in heifers. The frequency of AI increased significantly from 1.6 times (average of negative cows) to 3.4 times (average of positive cows). The first calving age was prolonged approximately 2 months, from 25.7 to 27.4 months (Table 2, $P<0.05$).

Table 2. Comparison of reproduction scores between seropositive and seronegative cows

Multiparous cows	Number of cows	NPT	AI	ELISA
Positive	20	16.0*	4.1*	0.59 ± 0.19
Negative	87	13.5	2.1	0.21 ± 0.04
Heifers	Number of cows	FC	AI	ELISA
Positive	5	27.4*	3.4*	0.65 ± 0.25
Negative	37	25.7	1.6	0.11 ± 0.01

AI: frequency of artificial insemination (average), *: $P<0.05$. NPT: average of non-pregnant terms (month) in multiparous cows. FC: average of first calving age in heifers, ELISA: the data are expressed as mean ± SD.

DISCUSSION

The seroprevalence of BDV in cows from the farm was 16.8%. The positive rate was higher in multiparous cows (18.7%) than in heifers (11.9%). The results were similar to a previous report in the Hokkaido region [8]. The frequency of AI in the seropositive cows increased to 4.1 times (average), implying a repeat bleeder. A repeat breeder was defined as a cow that did not become pregnant after 4 inseminations, despite no clinically detectable reproductive disorders [1]. The reproduction records of the seropositive cows showed no evidence of infection, leading to fertilization failure in the past 2 years. The estrus cycle appeared normal, even in the seropositive cows. There was no bias for the skill of AI practice among the cows, since one practitioner performed all AI procedures in this farm. The amount of feed was calculated by a program based on the milk production and body condition, and there was no deficiency in nutrients or quality.

Several studies have described the factors responsible for repeat breeding, such as environment, nutrition, and microorganisms [1, 2]. It is interesting that fertilization failure was also observed in seropositive heifers under nutrition management. All heifers were clinically normal, and their estrus cycles appeared normal. Infection by microorganisms is a cause of repeat breeding, but no particular microorganism that causes fertilization failure has been observed in this heard for the past 2 years.

In this study, we cannot elucidate the mechanism of fertilization failure in seropositive cows. However, an obvious reduction in breeding was observed in the seropositive cows. In our previous study, BDV RNA could be detected in a specific region of the brain from seropositive horses, but not in the uterus or ovaries from those animals [7]. BDV infection in the central nervous systems may be a factor that influenced the functions of female genital organs and hormone production. It is necessary to examine the influence that BDV infection in the central nervous system has on conception and the pregnancy.

ACKNOWLEDGMENTS. We thank T. Miura, D.V.M., and H. Iwao, D.V.M., for their technical assistance. We wish to express gratitude to the late Dr. Koichi Miyoshi, who helped conduct this research. This study was partially supported by a Grant-in-Aid for Scientific Research from the Ministry of Education, Culture, Sports, Science and Technology of Japan.

REFERENCES

1. Ayalon, N. 1978. A review of embryonic mortality in cattle. *J. Reprod. Fertil.* **54**: 483–493. [CrossRef] [Medline]
2. Azawi, O. I., Omran, S. N. and Hadad, J. J. 2008. A study of endometritis causing repeat breeding of cycling iraqi buffalo cows. *Reprod. Domest. Anim.* **43**: 735–743. [CrossRef] [Medline]
3. Bahmani, M. K., Nowrouzian, I., Nakaya, T., Nakamura, Y., Hagiwara, K., Takahashi, H., Rad, M. A. and Ikuta, K. 1996. Varied prevalence of Borna disease virus infection in Arabic, thoroughbred and their cross-bred horses in Iran. *Virus Res.* **45**: 1–13. [CrossRef] [Medline]
4. Hagiwara, K., Asakawa, M., Liao, L., Jiang, W., Yan, S., Chai, J., Oku, Y., Ikuta, K. and Ito, M. 2001. Seroprevalence of Borna disease virus in domestic animals in Xinjiang, China. *Vet. Microbiol.* **80**: 383–389. [CrossRef] [Medline]
5. Hagiwara, K., Kawamoto, S., Takahashi, H., Nakamura, Y., Nakaya, T., Hiramune, T., Ishihara, C. and Ikuta, K. 1997. High prevalence of Borna disease virus infection in healthy sheep in Japan. *Clin. Diagn. Lab. Immunol.* **4**: 339–344. [Medline]
6. Hagiwara, K., Matoba, Y. and Asakawa, M. 2009. Borna disease virus in Raccoons (*Procyon lotor*) in Japan. *J. Vet. Med. Sci.* **71**: 1009–1015. [CrossRef] [Medline]
7. Hagiwara, K., Momiyama, N., Taniyama, H., Nakaya, T., Tsunoda, N., Ishihara, C. and Ikuta, K. 1997. Demonstration of Borna disease virus (BDV) in specific regions of the brain from horses positive for serum antibodies to BDV but negative for BDV RNA in the blood and internal organs. *Med. Microbiol. Immunol. (Berl.)* **186**: 19–24. [CrossRef] [Medline]
8. Hagiwara, K., Nakaya, T., Nakamura, Y., Asahi, S., Takahashi, H., Ishihara, C. and Ikuta, K. 1996. Borna disease virus RNA in peripheral blood mononuclear cells obtained from healthy dairy cattle. *Med. Microbiol. Immunol. (Berl.)* **185**: 145–151. [CrossRef] [Medline]
9. Hagiwara, K., Okamoto, M., Kamitani, W., Takamura, S., Taniyama, H., Tsunoda, N., Tanaka, H., Iwai, H. and Ikuta, K. 2002. Nosological study of Borna disease virus infection in race horses. *Vet. Microbiol.* **84**: 367–374. [CrossRef] [Medline]
10. Hagiwara, K., Tsuge, Y., Asakawa, M., Kabaya, H., Okamoto, M., Miyasho, T., Taniyama, H., Ishihara, C., de la Torre, J. C. and Ikuta, K. 2008. Borna disease virus RNA detected in Japanese macaques (*Macaca fuscata*). *Primates* **49**: 57–64. [CrossRef] [Medline]
11. Ikuta, K., Ibrahim, M. S., Kobayashi, T. and Tomonaga, K. 2002. Borna disease virus and infection in humans. *Front. Biosci.* **7**: d470–d495. [CrossRef] [Medline]
12. Kishi, M., Nakaya, T., Nakamura, Y., Kakinuma, M., Takahashi, T. A., Sekiguchi, S., Uchikawa, M., Tadokoro, K., Ikeda, K. and Ikuta, K. 1995. Prevalence of Borna disease virus RNA in peripheral blood mononuclear cells from blood donors. *Med. Microbiol. Immunol. (Berl.)* **184**: 135–138. [CrossRef] [Medline]
13. Nishino, Y., Funaba, M., Fukushima, R., Mizutani, T., Kimura, T., Iizuka, R., Hirami, H. and Hara, M. 1999. Borna disease virus infection in domestic cats: evaluation by RNA and antibody detection. *J. Vet. Med. Sci.* **61**: 1167–1170. [CrossRef] [Medline]
14. Okamoto, M., Furuoka, H., Hagiwara, K., Kamitani, W., Kirisawa, R., Ikuta, K. and Taniyama, H. 2002. Borna disease in a heifer in Japan. *Vet. Rec.* **150**: 16–18. [CrossRef] [Medline]
15. Okamoto, M., Kagawa, Y., Kamitani, W., Hagiwara, K., Kirisawa, R., Iwai, H., Ikuta, K. and Taniyama, H. 2002. Borna disease in a dog in Japan. *J. Comp. Pathol.* **126**: 312–317. [CrossRef] [Medline]
16. Richt, J. A. and Rott, R. 2001. Borna disease virus: a mystery as an emerging zoonotic pathogen. *Vet. J.* **161**: 24–40. [CrossRef] [Medline]
17. Rott, R. and Becht, H. 1995. Natural and experimental Borna disease in animals. *Curr. Top. Microbiol. Immunol.* **190**: 17–30. [CrossRef] [Medline]
18. Staeheli, P., Sauder, C., Hausmann, J., Ehrensperger, F. and Schwemmle, M. 2000. Epidemiology of Borna disease virus. *J. Gen. Virol.* **81**: 2123–2135. [Medline]
19. Watanabe, Y., Yanai, H., Ohtaki, N., Ikuta, K. and Tomonaga, K. 2006. Prevalence of Borna disease virus antibodies in healthy Japanese black cattle in Kyushu. *J. Vet. Med. Sci.* **68**: 171–174. [CrossRef] [Medline]

BMC Research Notes

SHORT REPORT Open Access

Hepatitis E virus in Norway rats (*Rattus norvegicus*) captured around a pig farm

Yuta Kanai[1,4], Satoshi Miyasaka[1], Sachiko Uyama[1], Sachiyo Kawami[1], Yuko Kato-Mori[1], Muneo Tsujikawa[3], Mikihiro Yunoki[3], Shoko Nishiyama[1], Kazuyoshi Ikuta[2] and Katsuro Hagiwara[1*]

Abstract

Background: Hepatitis E virus (HEV) transmitted via the oral route through the consumption of contaminated water or uncooked or undercooked contaminated meat has been implicated in major outbreaks. Rats may play a critical role in HEV outbreaks, considering their negative effects on environmental hygiene and food sanitation. Although the serological evidence of HEV infection in wild rodents has been reported worldwide, the infectivity and propagation of HEV in wild rats remain unknown. To investigate if rats are a possible carrier of HEV, we studied wild Norway rats (*Rattus norvegicus*) that were caught near a pig farm, where HEV was prevalent among the pigs.

Methods: We examined 56 Norway rats for HEV. RNA from internal organs was examined for RT-PCR and positive samples were sequenced. Positive tissue samples were incubated with A549 cell line to isolate HEV. Anti-HEV antibodies were detected by ELISA.

Results: Sixteen rats were seropositive, and the HEV RNA was detected in 10 of the 56 rats. Sequencing of the partial *ORF1* gene from 7 samples resulted in partially sequenced HEV, belonging to genotype 3, which was genetically identical to the HEV prevalent in the swine from the source farm. The infectious HEVs were isolated from the Norway rats by using the human A549 cell line.

Conclusions: There was a relatively high prevalence (17.9%) of the HEV genome in wild Norway rats. The virus was mainly detected in the liver and spleen. The results indicate that these animals might be possible carrier of swine HEV in endemic regions. The HEV contamination risk due to rats needs to be examined in human habitats.

Background

Hepatitis E virus (HEV) is a causative agent of viral hepatitis transmitted via the oral route in humans. The clinical symptoms of HEV infection vary from asymptomatic to acute fulminant hepatitis. In humans, pregnancy and underlying liver diseases are considered risk factors for severe cases of HEV [1,2] and high mortality rates have been reported among pregnant women [3-6]. Also, chronic hepatitis associated with HEV was recently reported in organ transplant recipients [7].

HEV is a non-enveloped single-stranded positive-sense RNA virus classified as the sole member of the genus *Hepevirus* in the family *Hepeviridae* [8]. The 7.2-kb genome of HEV is composed of 3 open reading frames (ORFs): ORF1 (a non-structural protein), ORF2 (a capsid protein), and ORF3 (accessory proteins associated with virion cellular protein kinase activity and virion release) [9-12].

HEVs associated with human hepatitis are classified into 4 genotypes [13]. Genotypes 1 and 2 of HEVs cause waterborne diseases, these genotypes are endemic in developing countries and cause outbreaks involving large populations [14,15]; meanwhile, genotypes 3 and 4 are generally considered zoonotic HEVs. Molecular analysis of the virus in patients and contaminated food provide evidence for direct food-borne transmission of the virus [16-18]. Recently, HEVs were detected in rabbits in China and rats in Germany; however, their infectivity to humans remains undetermined [19,20].

Epidemiological studies suggest that pigs are an important virus source of human HEV infections [21-25]. Many studies have shown that HEV infection

* Correspondence: k-hagi@rakuno.ac.jp
[1]School of Veterinary Medicine, Rakuno Gakuen University, Ebetsu, Hokkaido 069-8501, Japan
Full list of author information is available at the end of the article

occurs in many other animals in addition to pigs as evidenced by the detection of the HEV RNA or HEV-specific antibodies [19,26-28]. Although the prevalence of HEV-specific antibodies in wild rodents is well documented [28-31], there is only a single report of HEV isolated from rats in Europe [20]. Besides natural infection, a few cases of successful experimental infections of HEV genotype 1 to Wistar rats [32], HEV genotype 3 to Mongolian gerbils [33], and HEV genotype 4 to nude mice [34] have been reported. Although the transmission of the virus from wild rodents to domestic animals (e.g., pigs) is possible, the extent of this risk remains unknown [35]. To investigate whether rodents can serve as reservoirs of porcine HEV, we examined HEV infection in wild rats caught around a pig farm where HEV infection was prevalent. To determine whether wild rats are reservoirs of swine HEV, we performed viral genome detection by reverse transcription-polymerase chain reaction (RT-PCR), serological examination, and virus isolation in wild rats.

Methods

Animals

Norway rats (*Rattus norvegicus*) were caught, using commercial snap traps at 6 different locations, around a pig farm where HEV genotype 3 was prevalent among pigs (Hokkaido, Japan) [36]. The farm consists of three buildings. The capture locations surrounded 3 different buildings where the grow-finishing pigs (about 120 total head counts) were reared. Our previous study revealed that all the pigs were infected with HEV genotype 3. These studies were performed in accordance with the guidelines for the capture, handling, and care of mammals of the Mammalogical Society of Japan. All animal experiments were approved by the Rakuno Gakuen University Ethical Committee for Animal Experiment Regulation, Hokkaido, Japan (approved #VH21C10).

The power analysis used to calculate the number of animals required for the study was performed on the basis of the 95% confidence interval shown on the Raosoft® website (http://www.raosoft.com/samplesize.html). Because the prevalence rate of HEV infection in wild rodents was estimated to be approximately 10% [28-31], the values required for calculating the sample size were set as follows: infection rate, 10%; margin of error that determines the range of the 95% confidence interval, 5%; and confidence level that refers to the likelihood of 95% confident interval, 90%. The power analysis indicated the appropriate sample size to be 97 to obtain 10% HEV infection in rats with a 5% margin of error. Since we found a sufficient number of HEV infections in rats when 56 animals were examined, no further capturing was performed.

Sampling and RNA extraction

The liver, spleen, intestines, and blood were collected from 56 wild rats to determine the presence of HEV RNA. Tissue and serum samples were collected from each rat, and the samples were stored at -80°C until analysis. Blood was collected from the hearts of dead wild rats by using filter paper (Toyo Roshi; Advantec, Tokyo, Japan) according to the manufacturer's instructions. The filter paper was dissolved in 1 mL of phosphate-buffered saline (PBS) and subsequently diluted (1:25) to make serum samples. During tissue collection from wild rats, each dissection instrument was sterilized to avoid contaminating tissues with HEV RNA. Tissue samples (100 mg) were homogenized using zirconia beads with a TissueLyser (Qiagen GmbH, Hilden, Germany). Viral RNA was extracted from 100 mg of the tissue sample by using 1 mL of TRIzol reagent (Life Technologies Corp., Carlsbad, CA) according to the manufacturer's instructions. The final elution was carried out using 50 μL of RNase-free H_2O. The RNA extracted from HEV-infected (genotype 3) swine livers was used as a positive control.

ELISA

Anti-HEV antibodies were detected by ELISA with a commercial kit (Viragent HEV-Ab kit; Cosmic Corporation, Tokyo, Japan) that used a truncated recombinant HEV ORF2 protein expressed in silkworm pupae [37] according to the manufacturer's instructions. For the positive control serum, 3 Wistar rats were subcutaneously immunized with ORF2 antigen (100 μg/rat) 3 times every 2 weeks. The recombinant ORF2 protein was produced as a fusion protein with glutathione-*S*-transferase (GST) from the plasmid, pGEX-AC2.1, which encodes the ORF2 antigen (genotype 3). TALON Metal Affinity Resin (Clontech Inc., Palo Alto, CA) was used to purify the recombinant ORF2 protein. The sera from 5 intact Wistar rats were used as negative controls. The serum samples were diluted in buffer (1:100) and were incubated for 1 h at room temperature. Because the ELISA kit was developed for detecting human antibodies, an HRP-conjugated anti-rat IgG antibody (Zymed Inc., South San Francisco, CA) was used as the secondary antibody. After the secondary antibody reactions, 50 μL of TMB (3,3',5,5'-tetramethylbenzidine) (Kirkegaard & Perry Laboratories Inc., Baltimore, MD) was added; after 30 min incubation at room temperature, 50 μL of 2 M sulfuric acid was added to stop the reaction. The optical density at 450 nm (OD_{450}) was measured. The cutoff value for IgG ELISA was calculated as the mean OD + 3 SDs of 5 uninfected Wistar rats (cutoff: OD 0.3).

RT-PCR and sequence analysis

Initially, the HEV RNA of the 5' terminal region of ORF1 was detected by semi-nested RT-PCR [36] with the sense primer HE61 (5'-CACRTATGTGGTCGAYGCCATG-GAG-3'; R = A or G, Y = C or T) and the antisense primer HE51 (5'-GCCKRACYACCACAGCATTCG-3'; K = G or T) for reverse transcription (RT) and first round of PCR and the internal sense primer HE50 (5'-AAGGCTCCTGGCRTYACWAC-3'; W = A or T) for the second round of PCR to confirm the first round of PCR products. Reverse transcription and first-round amplification were carried out using the OneStep RT-PCR Kit (Qiagen). In each reaction, 5-μL aliquots of viral RNA solution were used. The reactions were performed in an Eppendorf Mastercycler (Eppendorf, Hamburg, Germany) under the following conditions: RT at 50°C for 30 min, denaturation at 95°C for 15 min; 45 cycles of denaturation at 95°C for 15 s each, annealing at 55°C for 30 s, and elongation at 72°C for 30 s; and final extension at 72°C for 7 min. After the first round of PCR, 1-μL PCR product was amplified under the following conditions: 20 cycles of denaturation at 95°C for 15 s each, annealing at 60°C for 30 s, and elongation at 72°C for 15 s, followed by a final incubation at 72°C for 7 min. The amplified second-round PCR products were confirmed by 2% gel electrophoresis. The expected amplicon sizes of ORF1 were 125 bp and 85 bp in the first- and second-round PCRs, respectively. The RT-PCR-positive samples were also confirmed by semi-nested RT-PCR for the ORF 2 region by using the sense primer HE169 (5'-GAGGAG-GAGGCTACTTCCG-3') and the antisense primer HE 171 (5'-CAGCCGACGAAATCAATTCTGTCG-3') for the RT and first-round PCR, and for the semi-nested PCR primer HE170 (5'-GTAATGCTTTGCATT-CACGGCTCC-3'). The expected amplicon sizes of ORF2 for the first- and second-round PCRs were 373 bp and 349 bp, respectively. A 349-bp PCR amplicon was determined to be specific to HEV.

The PCR products from 7 positive samples (3 spleens and 4 intestines from 6 rats captured at 6 different locations) were excised from the gel, purified using QIAquick Gel Extraction Kit (Qiagen) and sequenced to confirm the specificity of the RT-PCR reaction. The purified products were cloned into a plasmid (pTA2, Cat: TAK-101; Toyobo Co. Ltd., Osaka, Japan) and sequenced using the M13 forward and reverse primers. The genomic sequences of the 5' terminal region of HEV ORF1 were compared using Bio Edit (version 7.0.9.0) (http://www.mbio.ncsu.edu/BioEdit/bioedit.html).

Virus isolation from wild Norway rats

To isolate infectious rat HEVs, both the spleens and intestines of 3 of the HEV-positive wild rats (#38, #49, #50) were homogenized, filtered through a 0.22-μm Millipore filter (Millipore, MA), and inoculated into A549 cells (human alveolar basal epithelial cells), which are sensitive to HEV infection [38-40]. After adsorption for 60 min, the cells were washed with PBS and cultured in DMEM (Sigma-Aldrich Corp., St. Louis, MO) containing 2% fetal bovine serum and insulin-transferrin-selenium-X supplement (Cat. 51500-056; Life Technologies Corp., Carlsbad, CA) at 37°C in a 5% CO_2 incubator [40]. The cells were passaged 3 days post-infection (dpi) and cultured in the same medium conditions. At 7 dpi, viral RNA was extracted from culture supernatants and cells by using a QIAamp Viral RNA Mini Kit (Qiagen). HEV RNA was examined by semi-nested RT-PCR for the ORF1 region as described above.

Immunofluorescence assay

HEV antigen was detected by immunofluorescence assay to confirm the infectivity of rat HEV. Virus-infected cells (7 dpi) fixed with acetone-methanol for 5 min were washed with PBS and reacted with pig anti-HEV polyclonal antibody purified from pigs infected with HEV genotype 3 [41]. After incubation for 60 min at room temperature, the cells were washed with PBS containing 0.1% Tween 20 and reacted with FITC-rabbit anti-porcine IgG (Zymed) for 60 min at room temperature. After washing with the buffer, stained cells were examined under a Zeiss Pascal confocal microscope (LSM 5; Carl Zeiss AG, Oberkochen, Germany).

Results

We captured 56 wild Norway rats at 6 different locations around a pig farm where HEV was detected among the pigs. Anti-HEV-specific antibodies in wild rats were examined by ELISA; 16 of the 56 (28.6%) rats were seropositive. HEV RNA ORF1 was detected in 10 of the 56 rats by semi-nested RT-PCR (17.9%): 5 in the spleen, 5 in the intestines, and 1 (rat ID #49) in both. HEV RNA at the ORF2 region was also detected in all of the HEV-RNA (ORF1)-positive samples. Six of the 10 RT-PCR-positive rats were seropositive in ELISA (Table 1). To confirm the specificity of the RT-PCR reaction, PCR products were purified and sequenced. These PCR products were obtained from tissues samples of rats captured at different locations, 3 spleens (#36, #38, and #49) and 4 intestines (#27, #43, #49, and #50). The nucleotide sequences of the partial ORF1 region of rat and swine HEV were closely related (swJB-M8, DDBJ: AB481228). Swine HEV genotype 3 (swJB-M8) was isolated from pigs in the same farm where rat HEV was isolated [42]. All 7 nucleotide sequences from the rats were similar and exhibited the greatest similarity to HEV genotype 3 (swJB-M8, 95.2-100%) followed by genotype 1 (81.8-88.6%), genotype 4 (77.2-84.1%), rabbit HEV-like virus (79.5%), genotype 2

(77.3%), avian HEV-like virus (68.2-70.5%), and rat HEV-like virus (56.8%).

To examine if the wild rats were carrying infectious HEV, we infected A549 cells with both splenic and intestinal homogenates from 3 HEV-positive rats (#38, #49, and #50). Although no apparent cytopathic effects were observed in A549 cells after inoculation, HEV RNA was detected in all samples by RT-PCR from both the supernatants and cells at 7 dpi. The presence of HEV antigen in the A549 cells was confirmed by immunofluorescence assay by using pig anti-HEV polyclonal antibodies (Table 1 and Figure 1).

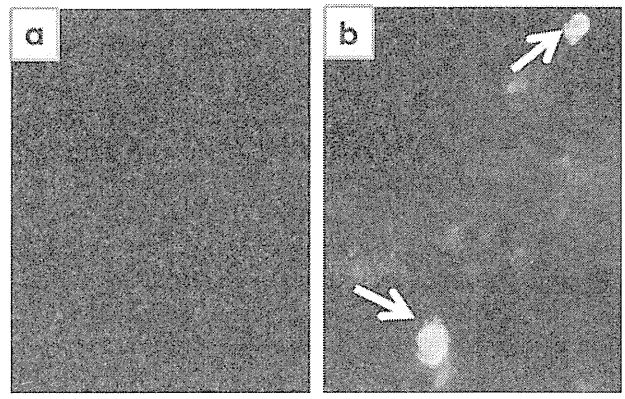

Figure 1 Detection of HEV-infected cells by immunofluorescence assay. a A549 cells of uninfected negative controls. **b** HEV-specific antigens were detected in A549 cells infected with splenic homogenate from rat #38.

Discussion

More than 40% of all rats from different regions of the United States are reported to be seropositive for HEV [43]. Rats may be infected with HEV after coming in contact with infected domestic animals or contaminated sewage. Epidemiological studies indicate that HEV infection in pigs is ubiquitous and that most pigs older than 3 months are seropositive [44-46]. Although HEV shedding in feces is observed in pigs of all ages, it is more frequently observed in 2- to 4-month-old pigs than in slaughter-age (6-month-old) or adult pigs [23,47-50]. In this study, we found several rat nests around the farm; the rats also often moved through the pig pens. Therefore, rats can easily infect HEV by coming in contact with contaminants.

There are many studies on the presence of an anti-HEV-specific antibody in wild rodents, including the reports on the detection of an HEV-like virus from Norway rats in Germany [20,51]. In this study, the partial sequence of HEV from rats was closely related to the swine HEV genotype 3 (swJB-M8). HEV RNA was detected not only in the intestines but also in the spleens of these rats, suggesting that HEV infects and replicates in wild rats. In this study, HEV RNA was not detected in liver samples. It is possible that RNA was rapidly degraded postmortem in this tissue. In addition, it is possible that only a small quantity of HEV was present in the samples.

Norway rats live, to great extent, in close association with humans. Although the dynamics of HEV in wild rats is unclear, there is a concern of the possibility of HEV spreading from rats to other species, including humans. Pigs are considered as the most important carrier of HEV because of the high prevalence of HEV among domesticated pig populations [36,44,45,48,50]. The fact that infectious HEV is found in pig manure [52] also emphasizes the importance of controlling HEV infection among pigs.

The risk factors for HEV infection are related to poor sanitation in endemic regions as well as HEV shedding in feces and subsequent water or food contamination in

Table 1 Summary of HEV RNA-positive Norway rats

Rat ID	Sex	Length (cm)	HEV-RNA			ELISA OD_{450}	Virus Isolation
			Liver	Spleen	Intestine		
11*	ND	ND	-	-	+	0.10	NT
27	Male	15	-	-	+	0.33	NT
36	Male	15	-	+	-	0.17	NT
38	Female	20	-	+	-	0.38	+
40	Male	20	-	+	-	0.30	NT
43	Female	15	-	-	+	0.30	NT
49	Male	19	-	+	+	0.39	+**
50	Male	18	-	-	+	0.68	+
51	Male	15	-	-	+	0.60	NT
53	Male	19	-	+	-	0.49	NT

* ND: the rat could not be measured because of sample damage

** HEV was isolated from both the spleen and intestines. NT: not examined